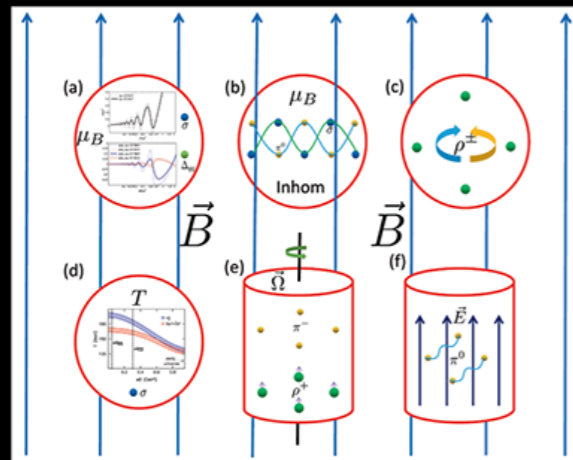


Topical Collection on The QCD Phase Diagram
in Strong Magnetic Fields

Edited by Pedro Costa, Débora Peres Menezes,
Vladimir Skokov and Carsten Urbach



From: Recent progresses
on QCD phases in a strong
magnetic field: views from
Nambu–Jona-Lasinio model
by Gaoqing Cao.
Figure permissions: a) Phys.
Rev. D 76, 105030 (2007),
d) JHEP 1202, 044 (2012).

The QCD phase diagram in strong magnetic fields

MAGNETIC FIELDS

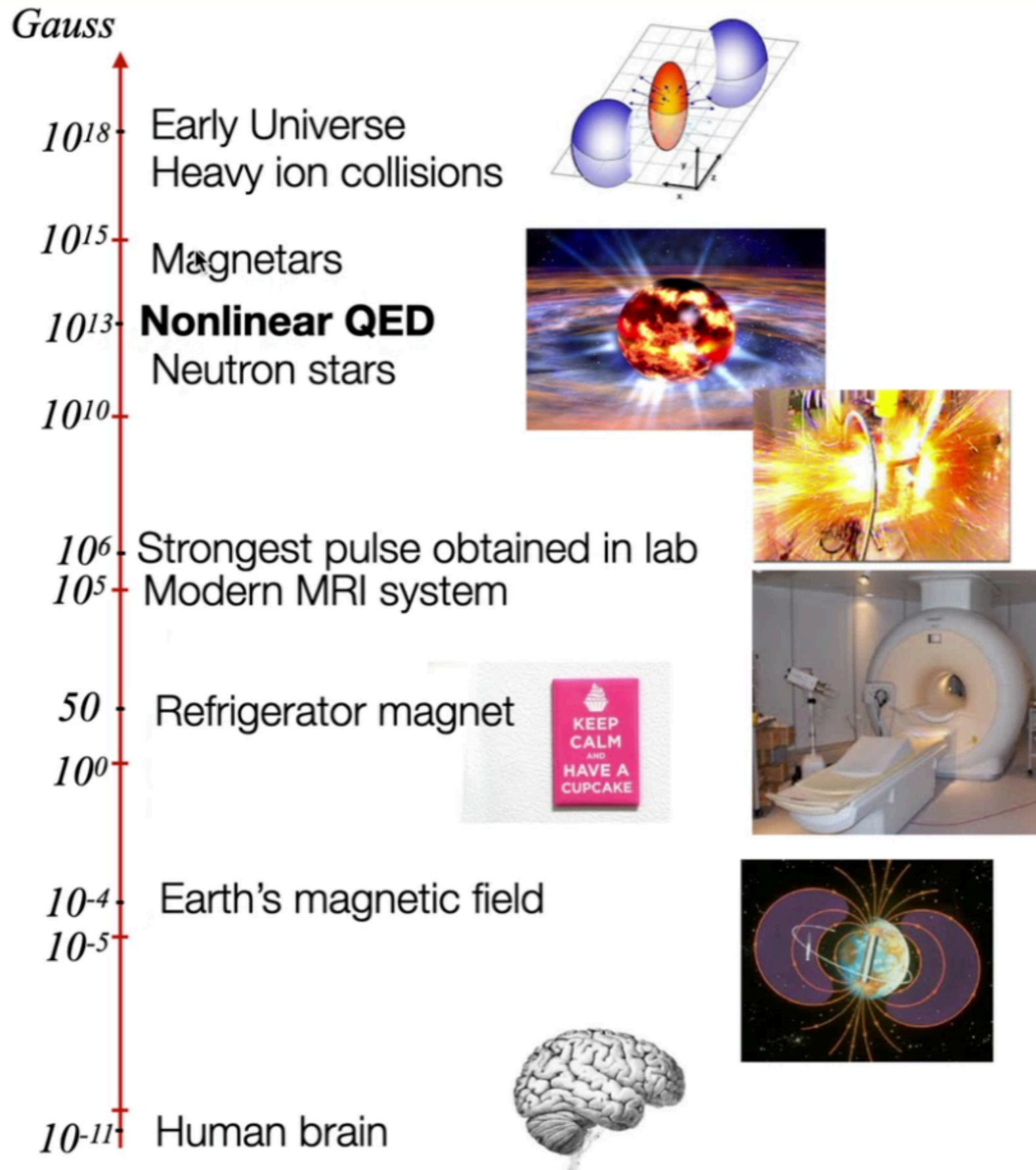
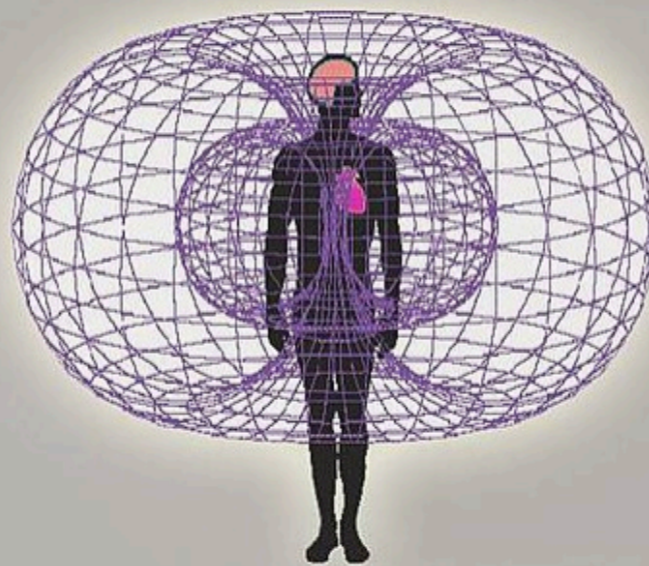


Figure taken from
Krill Tuchim's
seminar

Magnetocardiography (MCG) is a technique to measure the **magnetic fields** produced by electrical currents in the **heart** using extremely sensitive devices such as the **superconducting quantum interference device** (SQUID). If the magnetic field is measured using a multichannel device, a map of the magnetic field is obtained over the chest; from such a map, using mathematical **algorithms** that take into account the conductivity structure of the **torso**, it is possible to locate the source of the activity. For example, sources of abnormal rhythms or **arrhythmia** may be located using MCG.

Magnetocardiography

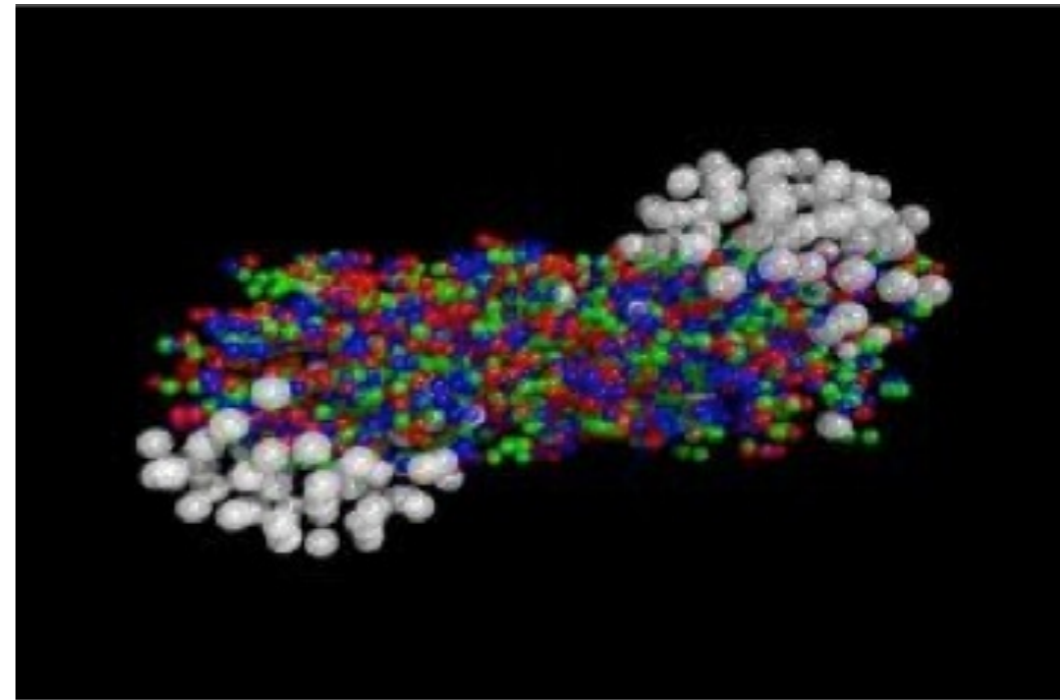
The electromagnetic field of the heart



The heart's electromagnetic field

Purpose records the magnetic fields generated by the heart

Motivation: why magnetic fields?



Magnetars - $eB \approx 0.5m_{\pi}^2$

$$m_{\pi}^2 \approx 3.5 \times 10^{18} \text{ G}$$

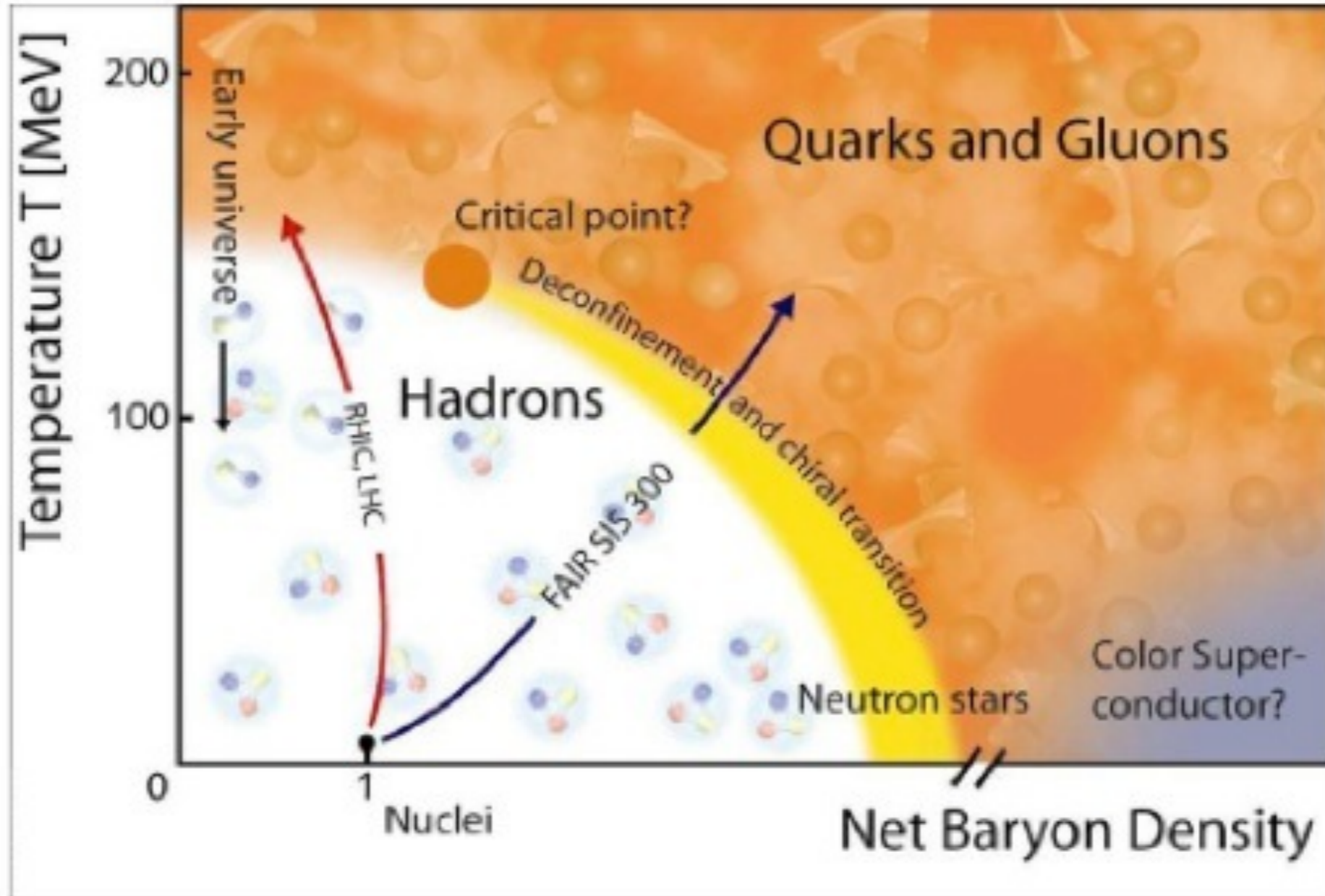
Non-central HIC - $eB \approx 5 - 15m_{\pi}^2$

Early Universe - $eB \approx 30m_{\pi}^2$

in natural units: $eB = 1 \text{ GeV}^2$ $B = 1.69 \times 10^{20} \text{ G}$

Heaviside-Lorentz, Gaussian and natural units lead to different conversions!

QCD Phase Diagram



What would happen if matter were subject to strong magnetic fields ?

We would like to understand magnetic field effects:

- at **high** densities and **low** temperatures (NS):
- at **low** densities and **high** temp. (heavy ion collisions);
- at **low** densities and **low** temperatures (pasta phase):
- if the **CEP** exists, how its **location** would change

CEP - NJL / PNJL

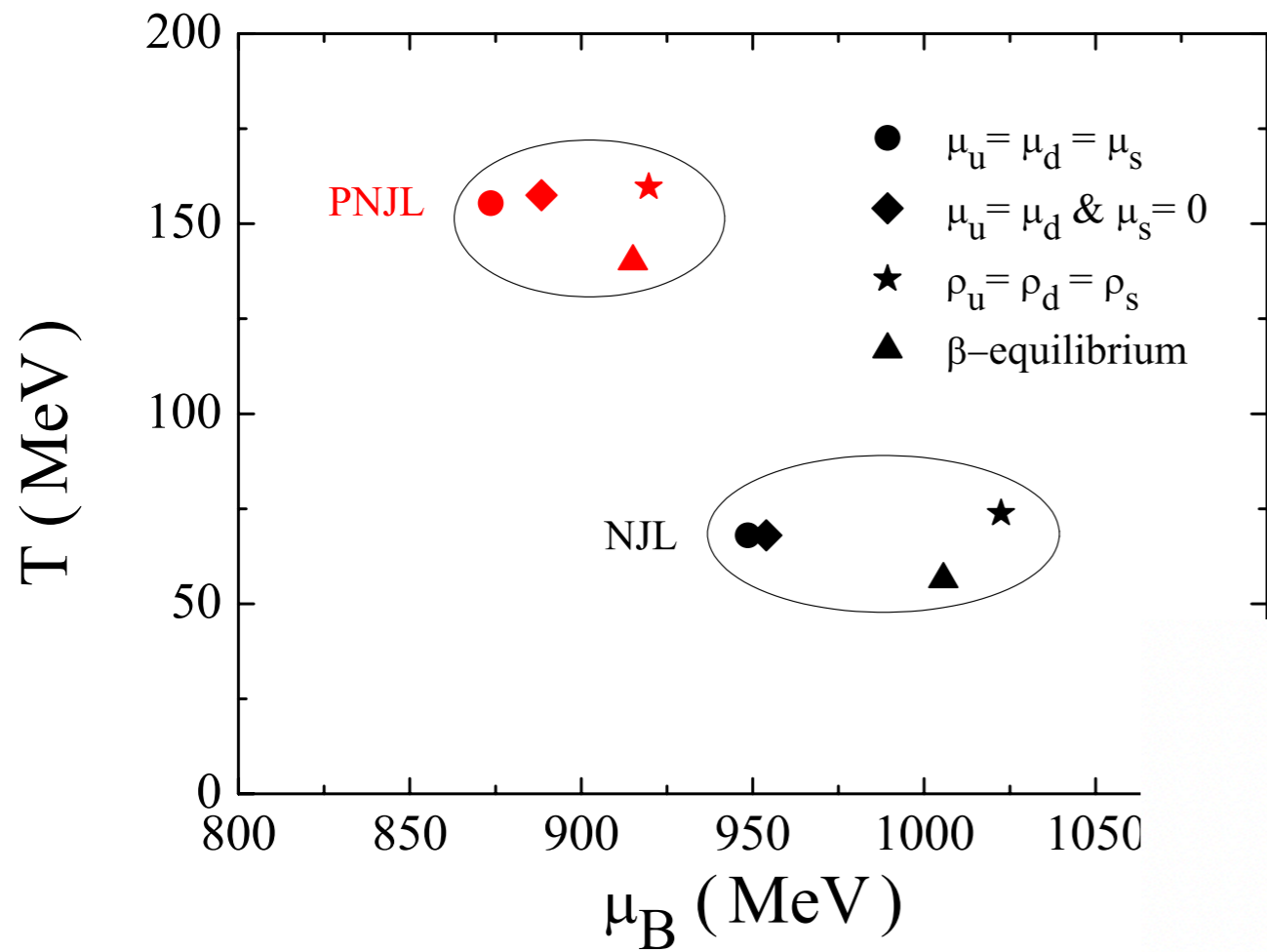
- **RKH parametrization / $B=0$ and strong B**
- **Different scenarios :**

$$\mu_u = \mu_d = \mu_s$$

$$\mu_u = \mu_d, \quad \mu_s = 0$$

- $\rho_u = \rho_d = \rho_s$

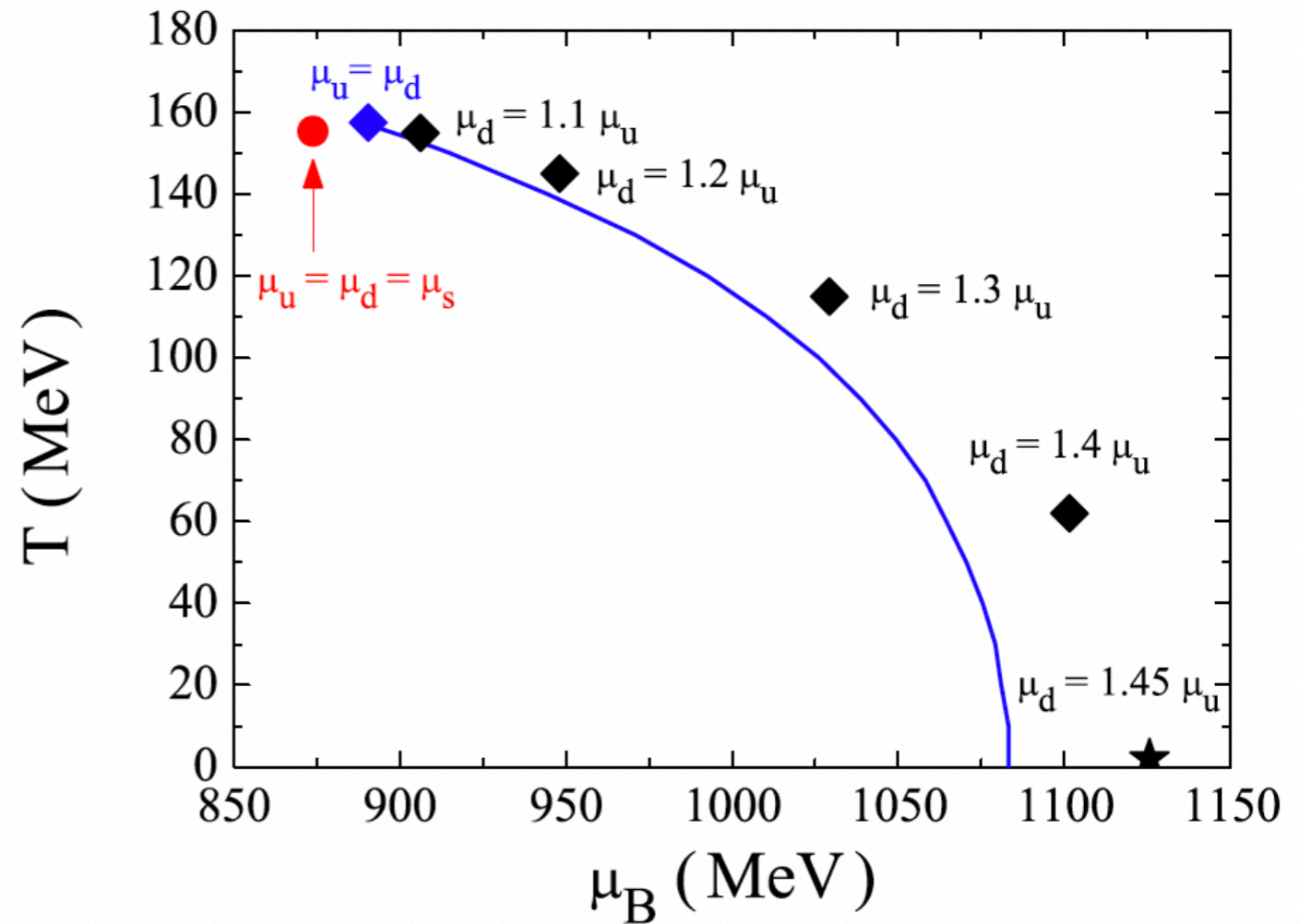
β – equilibrium

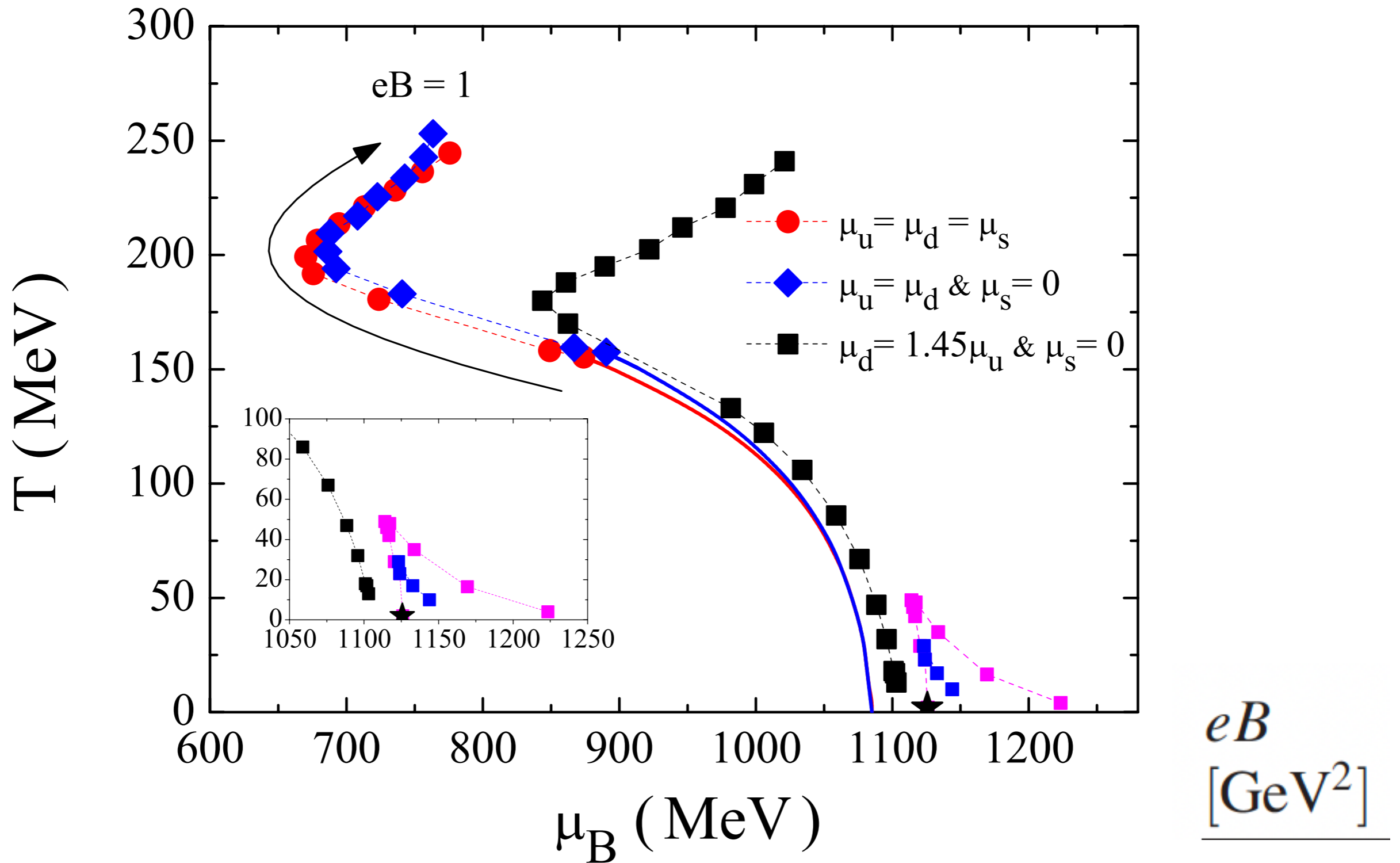


**Full line = zero isospin
PNJL**

$$\mu_u = \mu_d, \quad \mu_s = 0$$

B=0



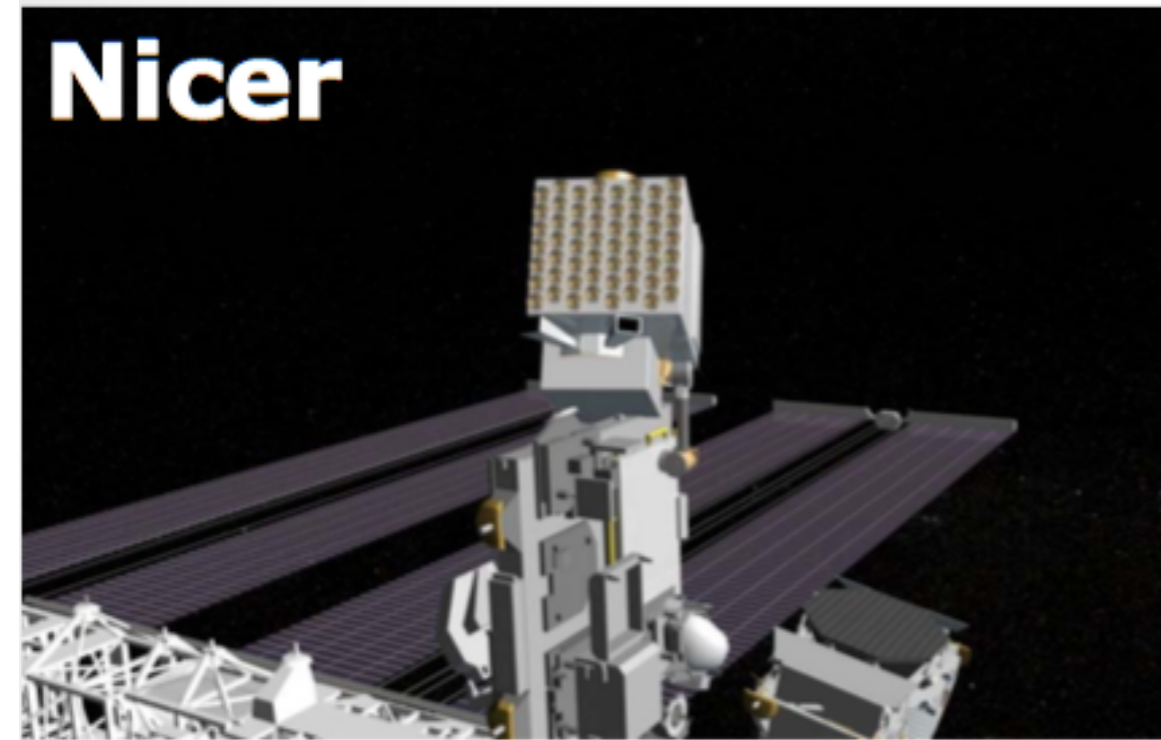


**Full lines= 1st order transitions at $eB=0$;
 two CEPs at low T and strong B (pink and blue)**

$$0.03 \lesssim eB \lesssim 0.07$$

NS interior composition explorer - 06/2017

Nicer



Main NS manifestations:

$$M = M_{\odot} \simeq 10^{30} \text{ Kg}$$

$$R \simeq 10 \text{ Km}$$

$$\rho = M/R^3 \simeq 10^{18} \text{ Kg/l}$$

- **Pulsars** - powered by rotation energy (1900 observed in radio-frequency)
- **Accreting X-Ray Binaries** powered by gravitational energy (rotation periods 0.0015-1000 s)

Athena



**Advanced telescope for high energy astrophysics
to be launched in 2030**

Magnetars don't fit into these categories! They are normally isolated NS whose main power source is the magnetic field.

There are 2 classes of magnetars (29):

<http://www.physics.mcgill.ca/~pulsar/magnetar/main.html>

- **Soft gamma-ray repeaters** (discovered in 1979 as transient X-ray sources and giant flares - 12 confirmed, 4 candidates);
- **Anomalous X-ray pulsars** (identified in 1990 as a class of persistent
- X-ray with no sign of a binary companion - 12 confirmed,
- 2 candidates);

The McGill Magnetar Catalog

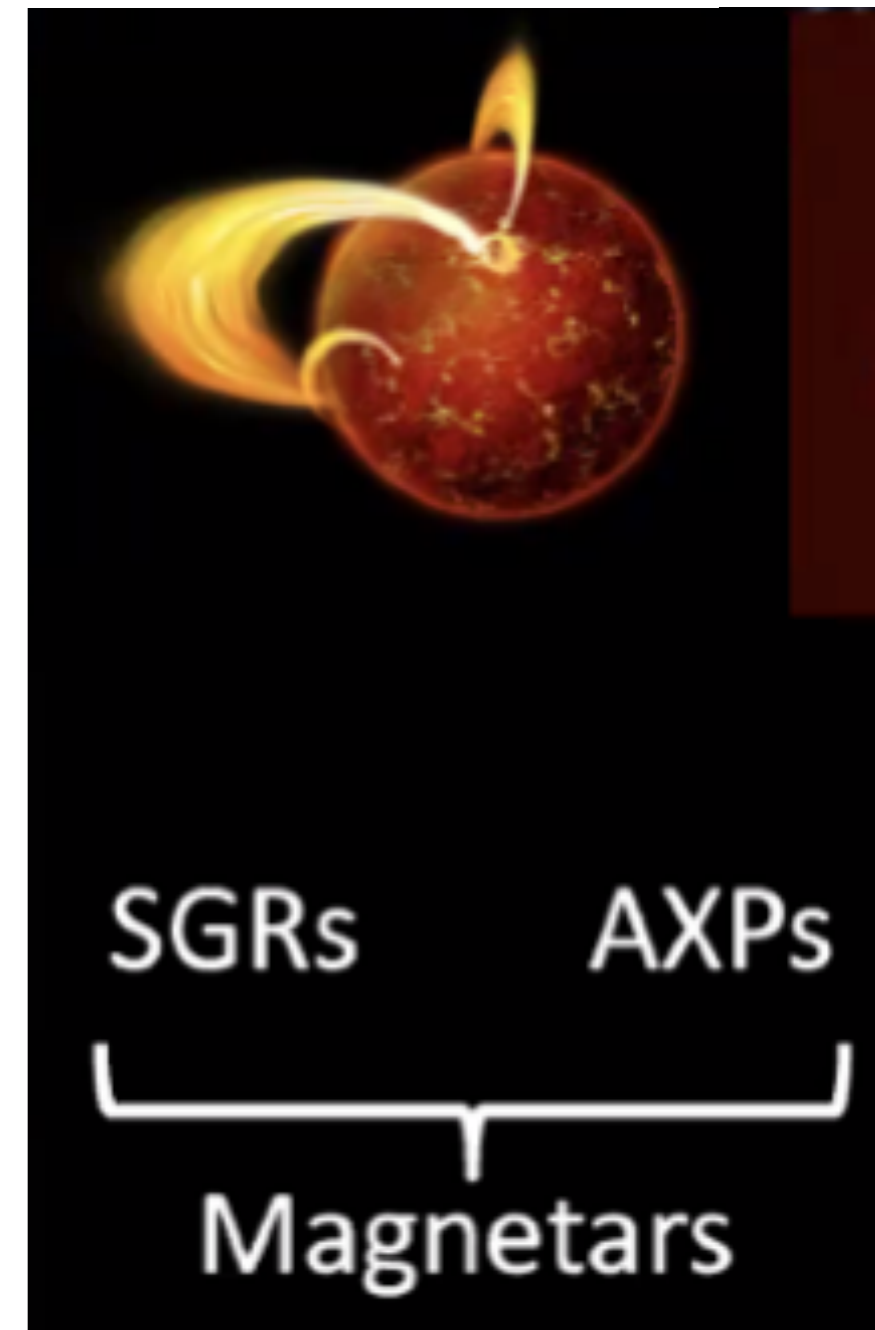
Show affiliations

Olausen, S. A. ; Kaspi, V. M.

So far, 30 magnetars:

16 SGRs (12 confirmed, 4 candidates)

14 AXPs (12 confirmed, 2 candidates)



Measuring Magnetic Fields of Neutron Stars

Rotation-powered NS

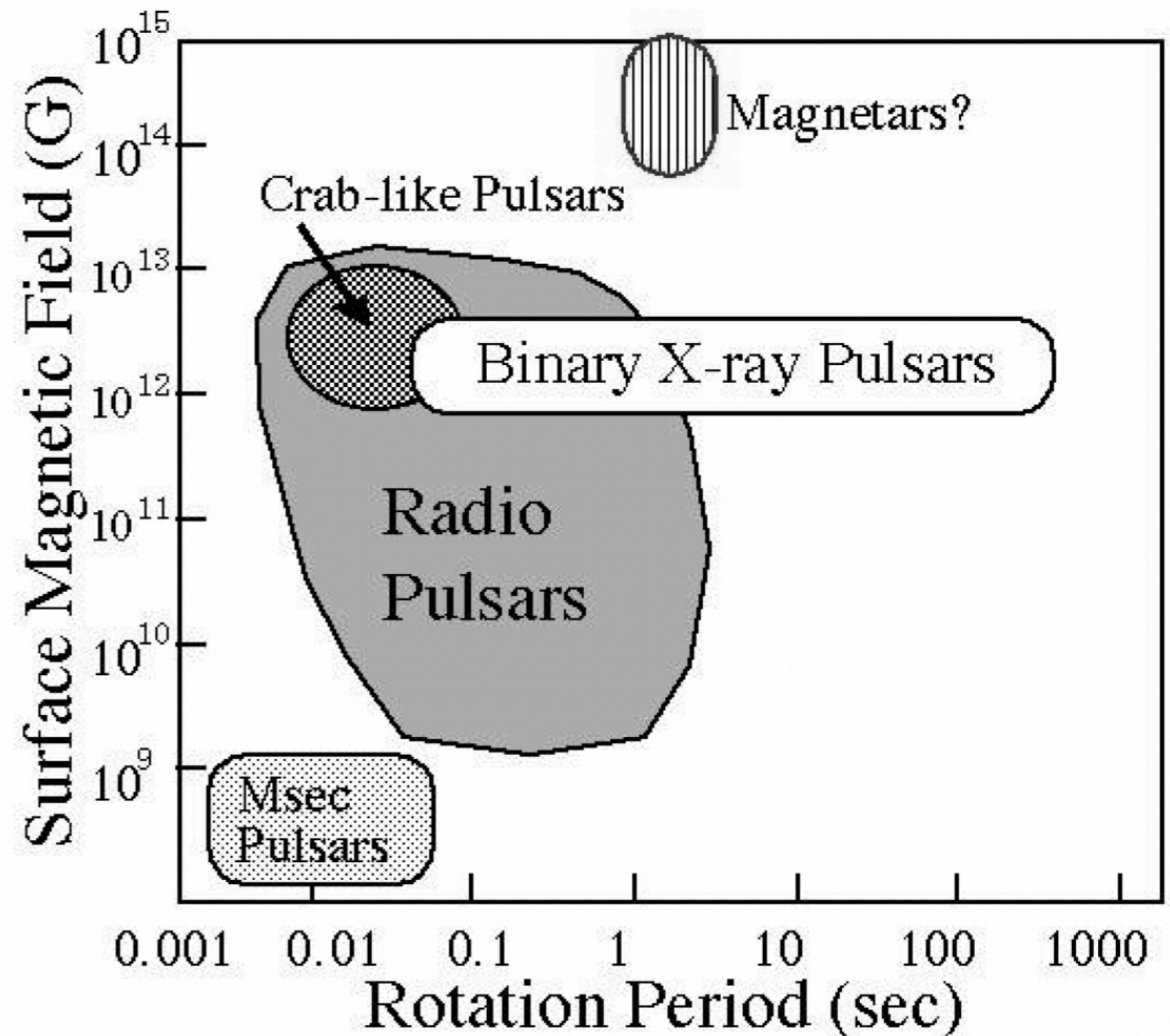
Spin down ->
decrease in rotational energy

Assuming decreasing is due
to magnetic dipole radiation:

$$B \propto \sqrt{P\dot{P}}$$

$$P = 2 - 12s$$

$$\dot{P} = 10^{-13} - 10^{-10}$$



🔒 | RESEARCH ARTICLE | STELLAR ASTROPHYSICS



A massive helium star with a sufficiently strong magnetic field to form a magnetar

[TOMER SHENAR](#) , [GREGG A. WADE](#), [PABLO MARCHANT](#) , [STEFANO BAGNULO](#) , [JULIA BODENSTEINER](#) , [DOMINIC M. BOWMAN](#) , [AVISHAI GILKIS](#) ,
[NORBERT LANGER](#), [ANDRÉ NICOLAS-CHENÉ](#) , [...], AND [SILVIA TOONEN](#)  [+6 authors](#) [Authors Info & Affiliations](#)

SCIENCE • 17 Aug 2023 • Vol 381, Issue 6659 • pp. 761-765 • [DOI: 10.1126/science.ade3293](https://doi.org/10.1126/science.ade3293)

<https://www.science.org/doi/10.1126/science.ade3293>

Un **magnétar** ou une **étoile magnétique**, une **magnétoile** selon la dénomination officielle en France¹, est une **étoile à neutrons** dont le **champ magnétique** est extrêmement intense et qui émet un **rayonnement électromagnétique** de haute énergie (**rayons X** et **rayons gamma**).

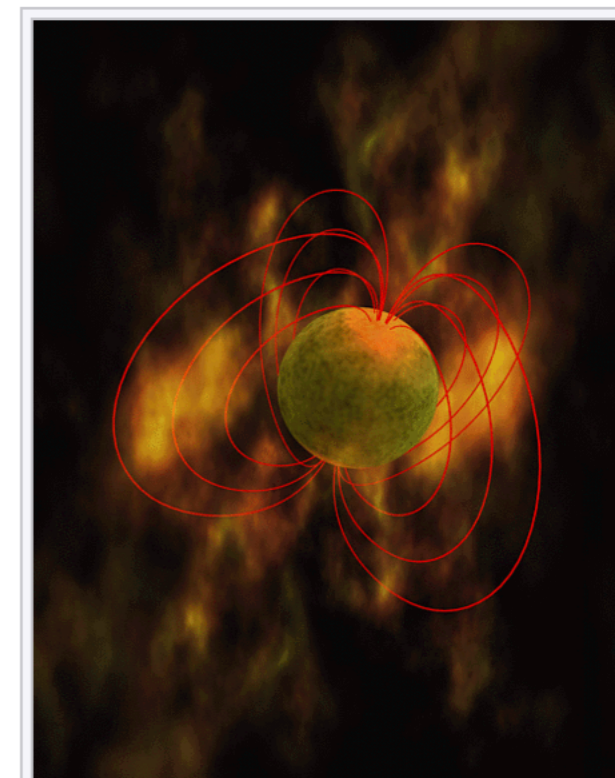
Histoire

[modifier | modifier le code]

L'existence des magnétars est postulée en 1992 par les astronomes **Robert Duncan** (en) et **Christopher Thompson** (de), qui établissent un lien entre la théorie des champs magnétiques intenses et les observations des sources gamma². Dans la décennie qui suit, elle est acceptée comme explication plausible des **sursauteurs gamma mous** et des **pulsars X anormaux**.

L'explosion du magnétar **SGR 1806-20** est enregistrée en 2004. L'énergie libérée a affecté l'atmosphère supérieure de la **Terre**, alors que celle-ci se trouvait à 50 000 **années-lumière** de l'explosion (ce qui veut dire que l'explosion a eu lieu il y a environ 50 000 ans).

En 2023, l'une des deux étoiles du **système binaire** HD 45166 est identifiée comme une **étoile Wolf-Rayet** ayant une masse de 2 **masses solaires** et un champ magnétique de 43 kG : selon les modèles d'évolution stellaire elle explosera en supernova et laissera comme résidu un magnétar. Cette étoile Wolf-Rayet fortement magnétique résulte vraisemblablement de la fusion de deux **étoiles à hélium** de masse inférieure³.



Vue d'artiste d'un magnétar.



Notes et références

[modifier | modifier le code]

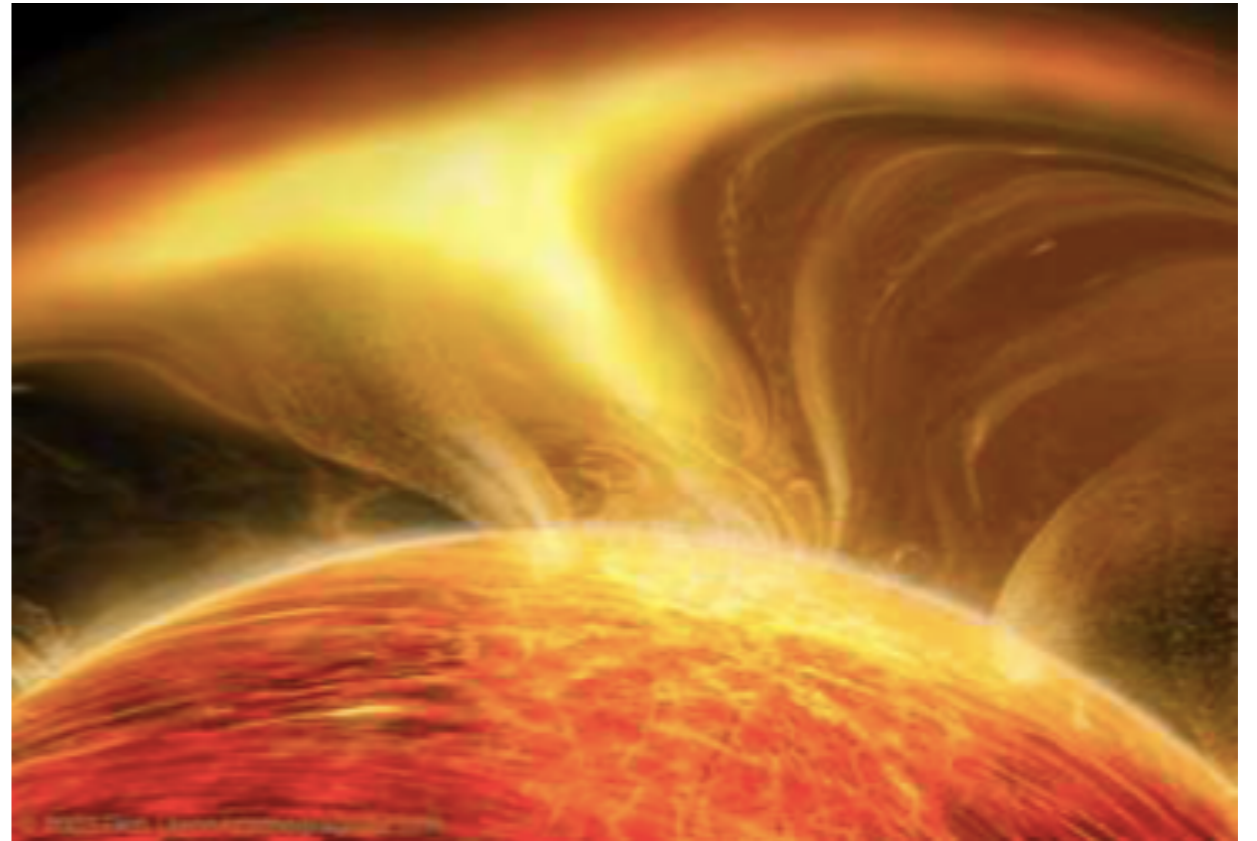
- ↑ (en) K. D. Marquez, M. R. Pelicer, S. Ghosh, J. Peterson, D. Chatterjee *et al.*, « Exploring the effects of Δ baryons in magnetars », *Physical Review C*, vol. 106, septembre 2022, article n^o 035801 (DOI [10.1103/PhysRevC.106.035801](https://doi.org/10.1103/PhysRevC.106.035801)).

Pulsars x Magnetars



Crab nebula pulsar/ Chandra

$$B = 10^{12} \text{ G}$$



Just my imagination

$$B = 10^{15} \text{ G}$$

But the EOSs are only sensitive to $B > 10^{17} \text{ G}$

Structure of a NS

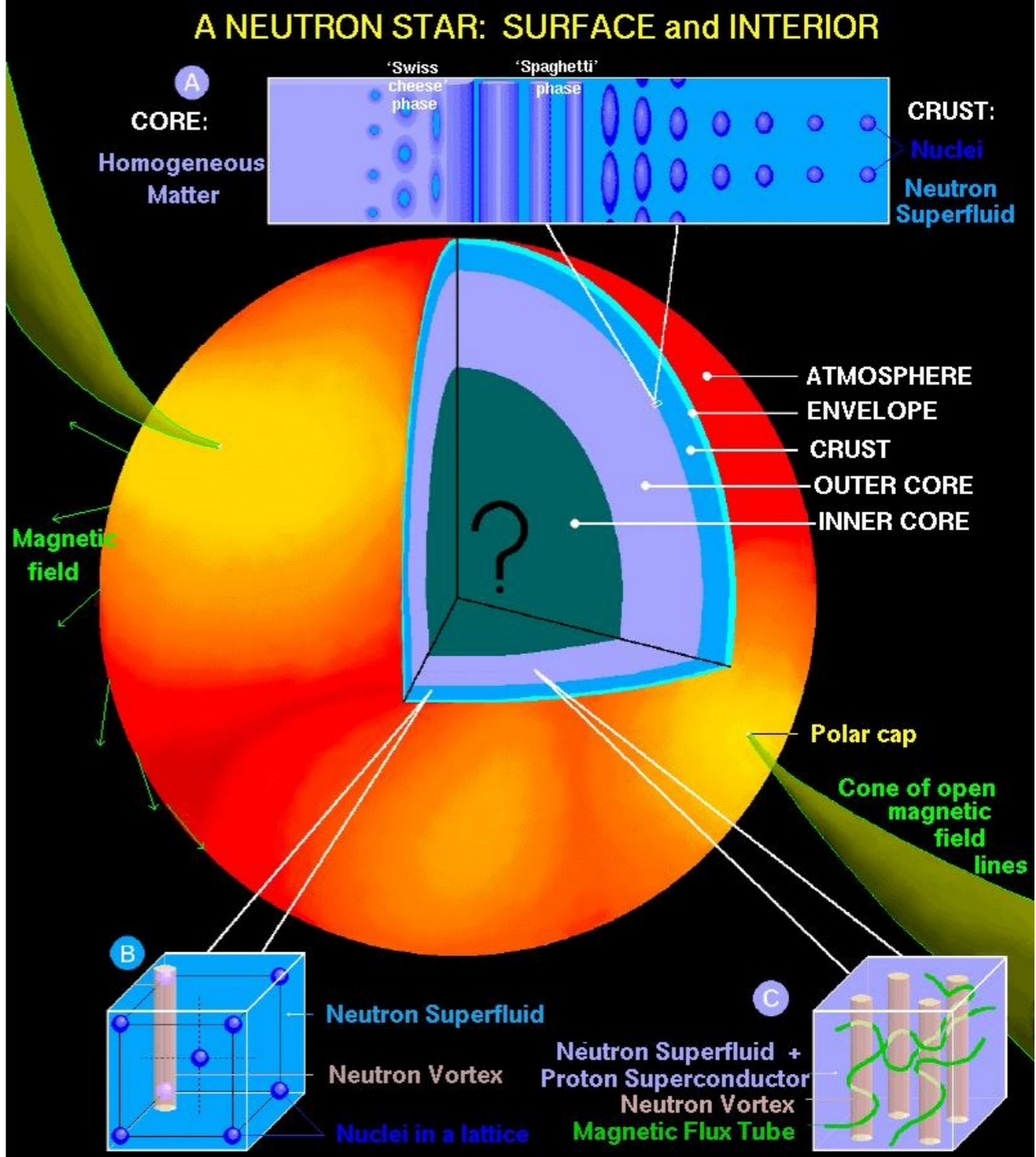
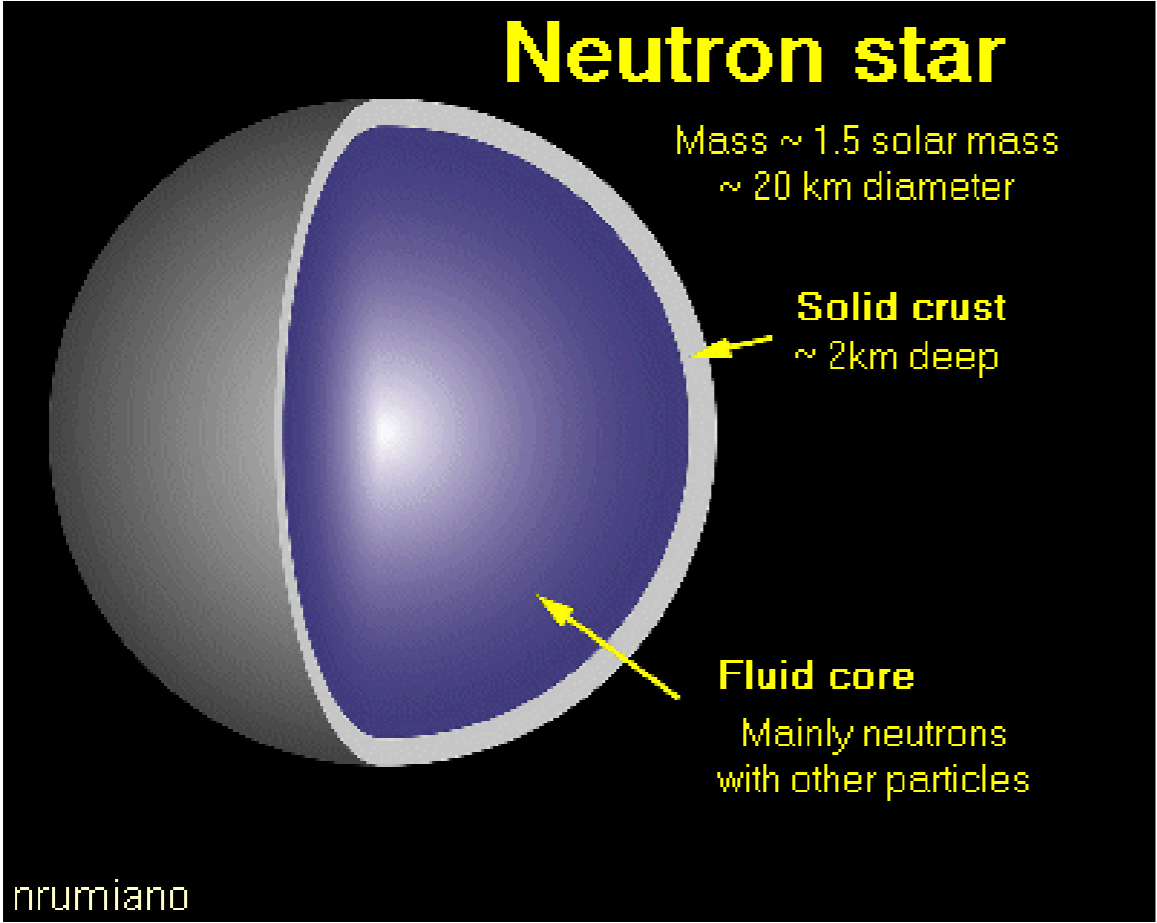


Figure by Danny Page

Liquid-gas phase transitions

Spinodal instabilities:

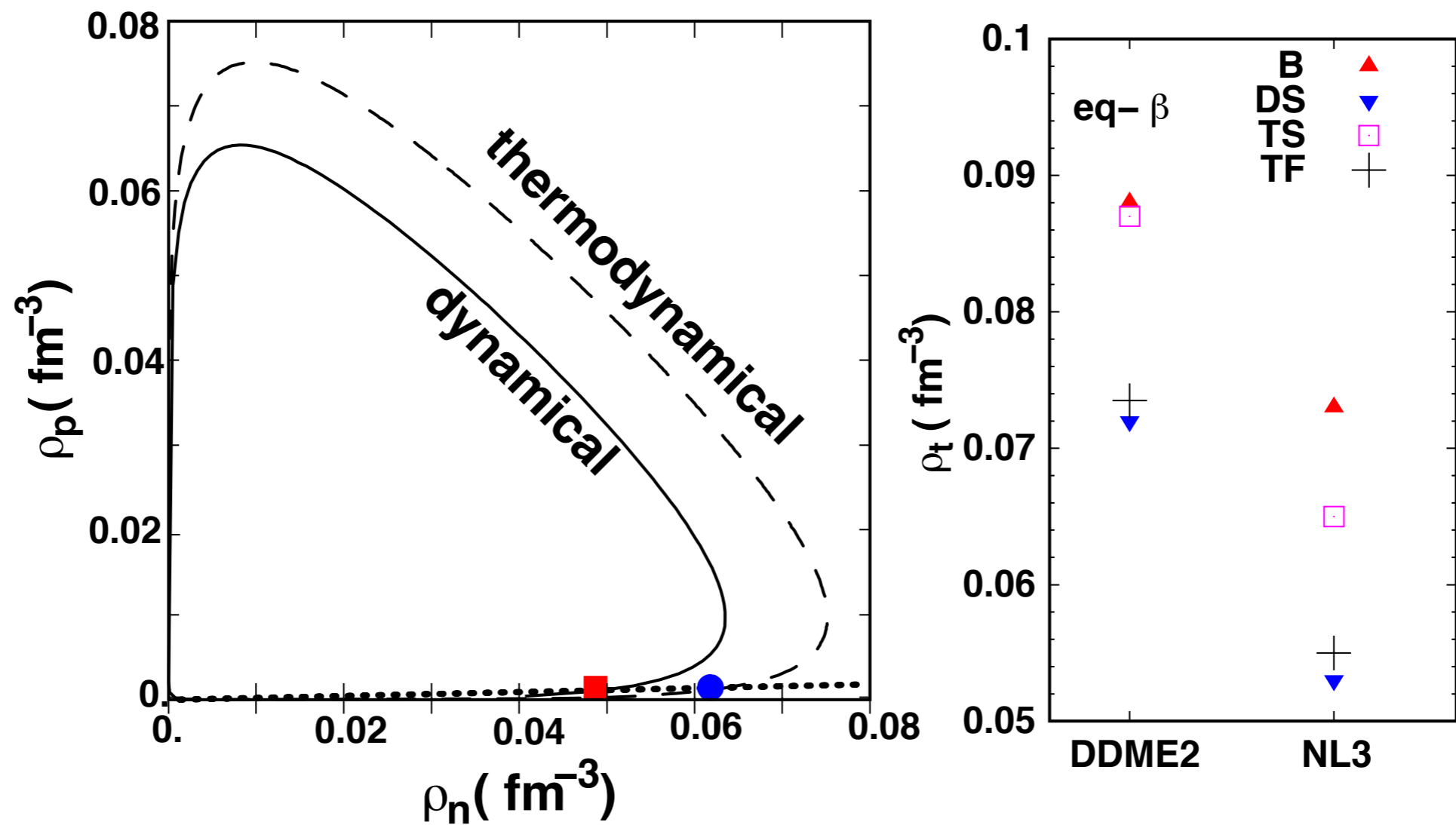
thermodynamical - obtained from the determinant of the symmetric matrix:

$$\mathcal{F}_{ij} = \left(\frac{\partial^2 \mathcal{F}}{\partial \rho_i \partial \rho_j} \right)_T,$$

dynamical - obtained from the Vlasov equation:

$$\frac{\partial f_{i\pm}}{\partial t} + \{f_{i\pm}, h_{i\pm}\} = 0, \quad i = p, n, e,$$

How to calculate crust-core transition density?



D. Chatterjee, F. Gulminelli and DPM, JCAP 03 (2019) 035

$$B^* = B/B^e$$

$$B^e = 4.4 \times 10^{13} G$$

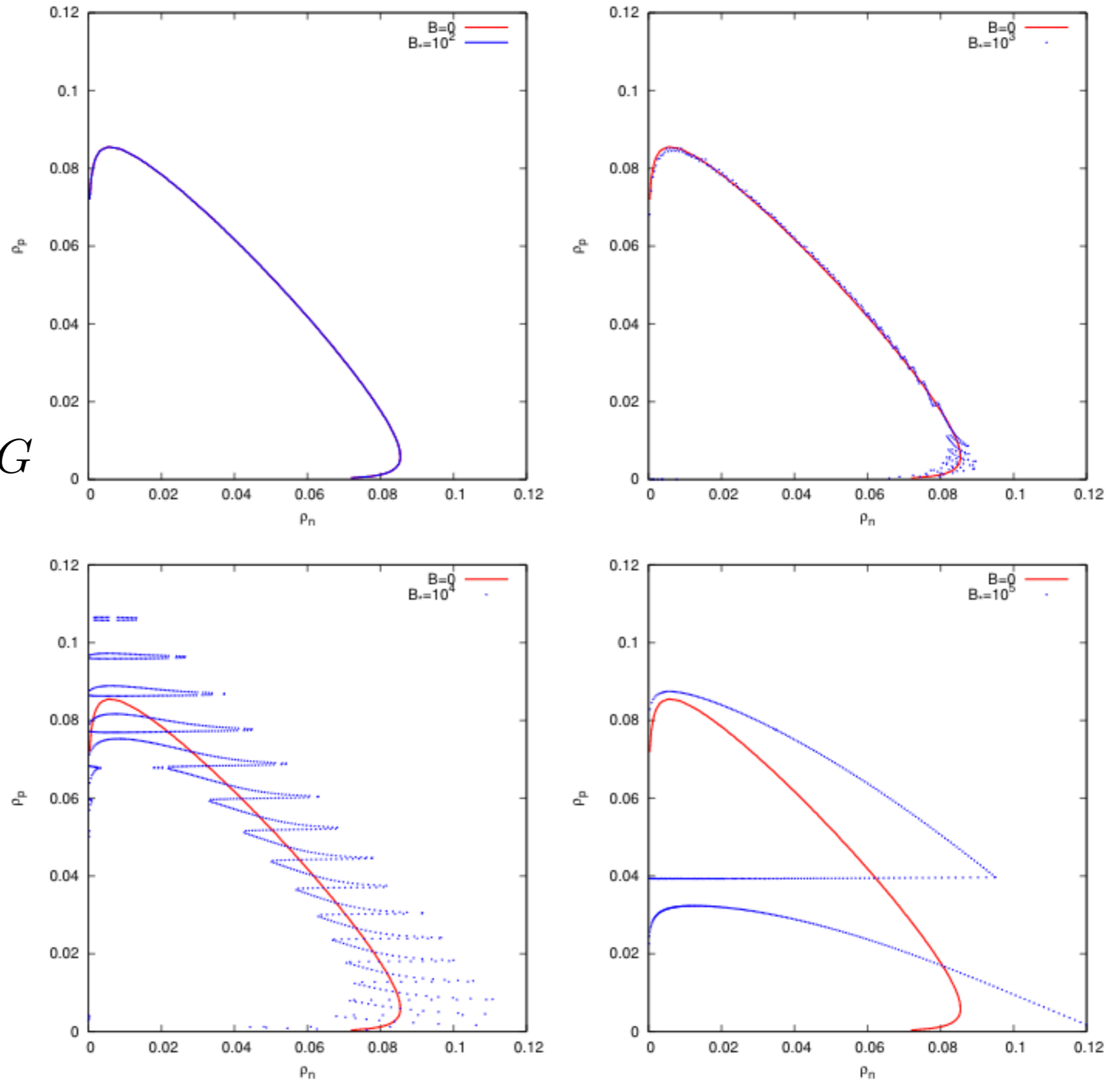


Figure 1: Thermodynamic spinodal for relative magnetic field strength $B_* = 10^2$ (upper left), 10^3 (upper right), 10^4 (lower left), 10^5 (lower right) B_c^e .

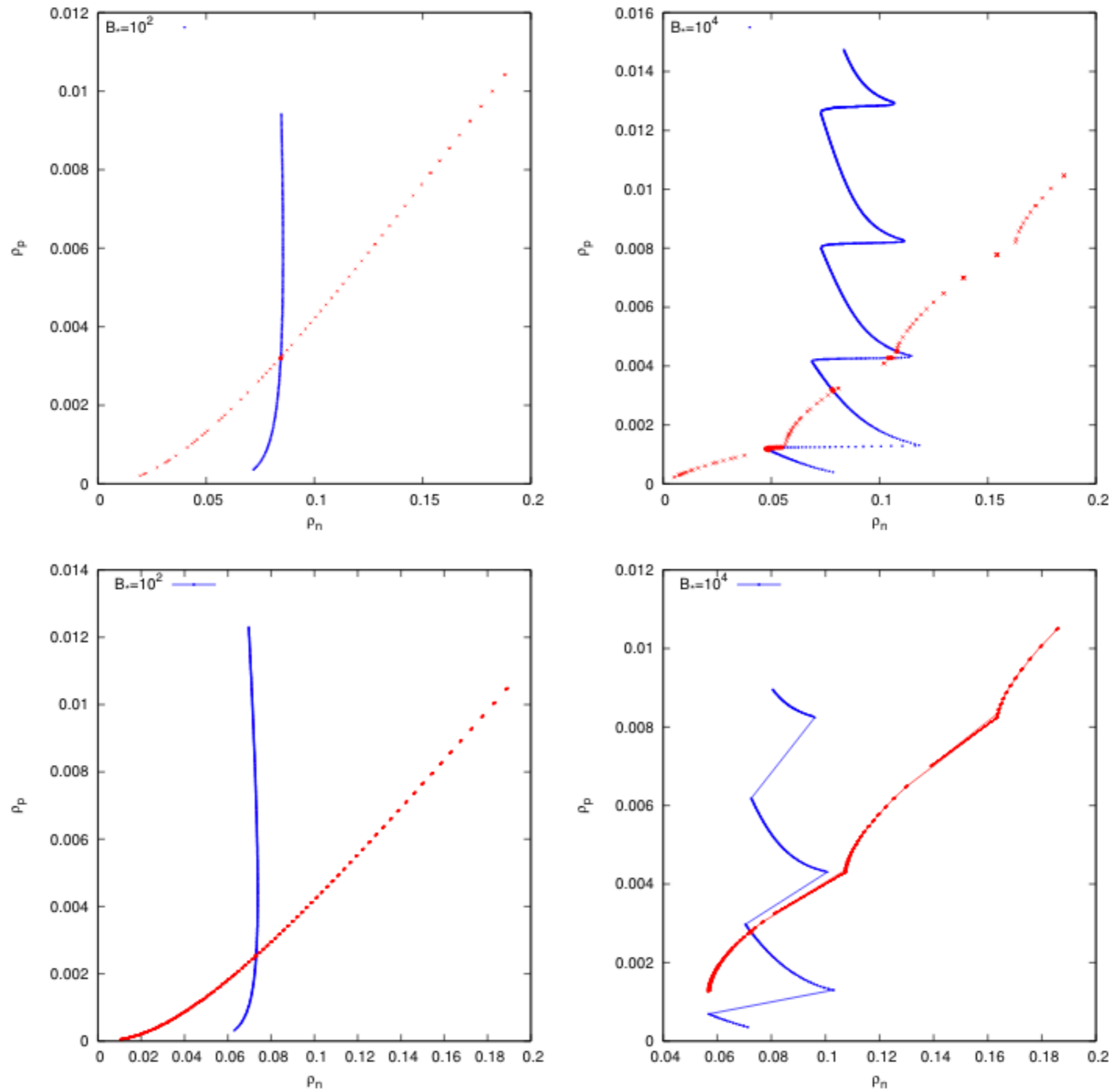


Figure 2: The crossing of the β -equilibrium line with the thermodynamic (upper panels) and dynamical (lower panels) spinodal for relative magnetic field strength $B_* = 10^2$ (left part) and 10^4 (right part) B_c^e . The Sly5 functional is used.

How can we obtain the crust thickness ?

One integrates from core to ccpt with **TOV** - core mass and radius

$$M_{crust} = \frac{4\pi P_{cc} R_{core}^4}{GM_{core}} \left(1 - \frac{2GM_{core}}{R_{core}c^2} \right)$$

$$R_{NS} = \frac{R_{core}}{1 - (\alpha - 1)(R_{core}c^2 GM_{NS} - 1)}$$

$$\alpha = (\mu_{cc}/\mu_0)^2, \quad \mu_0 = 930.4 \text{ MeV}$$

$$l_{crust} = R_{NS} - R_{core}$$

$$\Delta l_{crust} = l_{crust}^2 - l_{crust}^1$$

canonical star - Sly4 - isotropic EOS

B_*	ρ_1 (fm ⁻³)	R_{NS}^1 (km)	R_{core}^1 (km)	l_{crust}^1 (km)	ρ_2 (fm ⁻³)	R_{NS}^2 (km)	R_{core}^2 (km)	l_{crust}^2 (km)	Δl_{crust} (km)
0	0.077	11.704	10.797	0.908	0.077	11.704	10.797	0.908	0
10^2	0.076	11.771	10.843	0.928	0.076	11.771	10.843	0.928	0
10^3	0.071	11.770	10.859	0.911	0.074	11.770	10.849	0.920	0.009
5×10^3	0.070	11.764	10.865	0.899	0.084	11.761	10.8	0.961	0.062
7×10^3	0.033	11.804	10.993	0.811	0.081	11.777	10.811	0.966	0.155
10^4	0.041	11.826	10.97	0.856	0.074	11.795	10.855	0.940	0.084

expected crust size = of the order of 2.4 km (?)

J. Piekarewicz, F. J. Fattoyev and C.J. Horowitz, Phys. Rev. C 90, 015803 (2014)

TOV = small crust

LORENE = solves Einstein-Maxwell and equilibrium solutions self consistently with a magnetic field dependent EOS

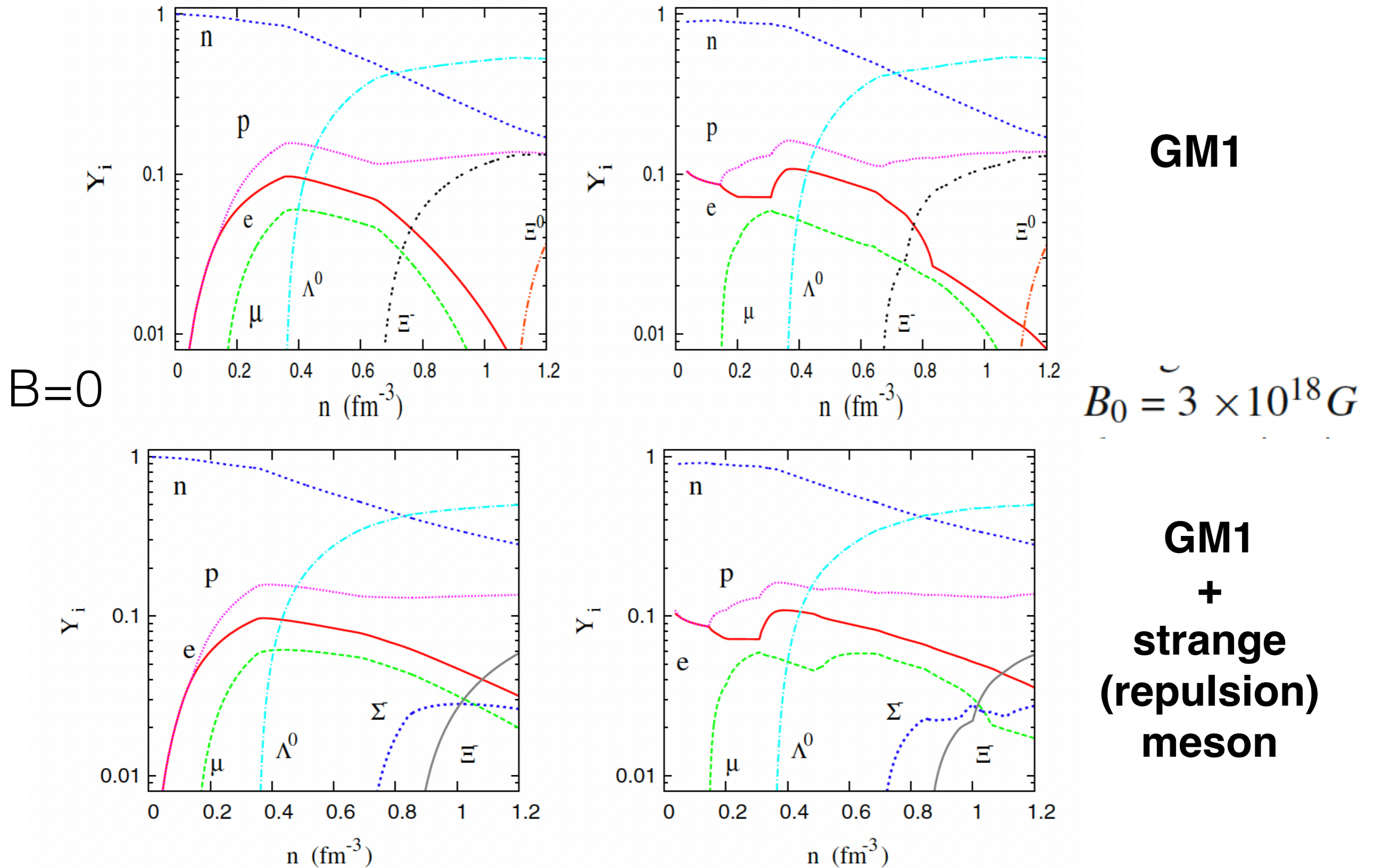
B_*	ρ_1 (fm^{-3})	R_{NS}^1 (km)	R_{core}^1 (km)	l_{crust}^1 (km)	ρ_2 (fm^{-3})	R_{NS}^2 (km)	R_{core}^2 (km)	l_{crust}^2 (km)	Δl_{crust} (km)
10^2	0.076	11.791	8.577	3.214	0.076	11.791	8.577	3.214	0
10^3	0.074	11.782	8.595	3.187	0.074	11.782	8.595	3.187	0
5×10^3	0.070	11.836	8.705	3.131	0.084	11.841	8.448	3.393	0.262
7×10^3	0.033	11.900	8.585	3.315	0.081	11.896	8.320	3.576	0.261
10^4	0.041	12.039	8.300	3.739	0.074	12.037	8.129	3.908	0.169

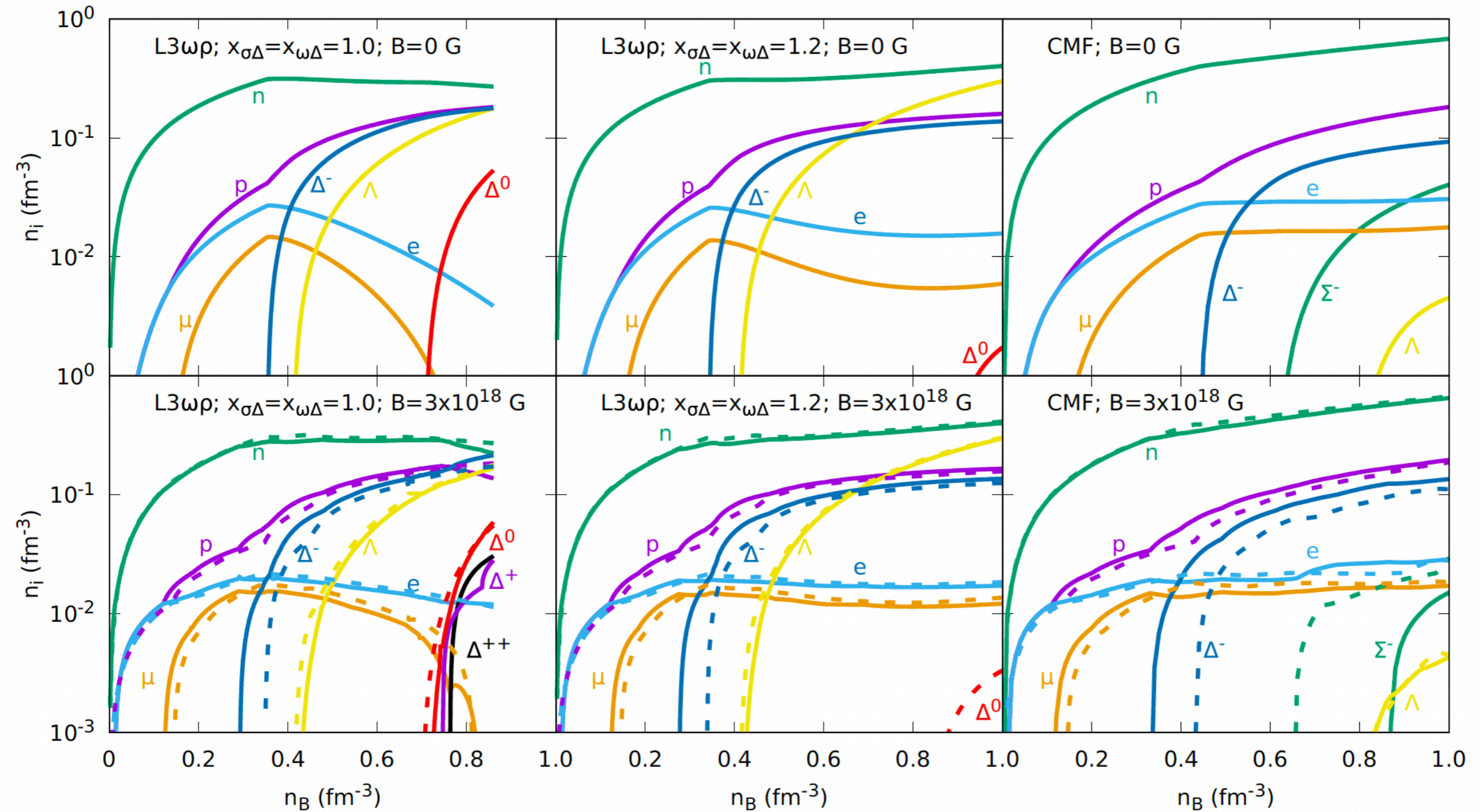
expected crust size = of the order of 2.4 km (?)

J. Piekarewicz, F. J. Fattoyev and C.J. Horowitz, Phys. Rev. C 90, 015803 (2014).

Lorene = large crust

What is the effect of B on the NS constituents?





Solid lines - without AMM; dashed lines - with AMM

K.D. Marquez, M.R.Pelicer, S. Ghosh, J.Petterson, D. Chatterjee, V. Dexheimer,
DPM, PRC 106, 035801 (2022)

Anisotropy in a Fermi gas

$$T^{\mu\nu} = T_{\text{matter}}^{\mu\nu} + T_{\text{fields}}^{\mu\nu}. \quad (1)$$

We consider a background magnetic field B pointing along the z -direction.

Be aware:

Heaviside-Lorentz units:

$$T_{\text{fields}}^{\mu\nu} = \text{diag}(B^2/2, B^2/2, B^2/2, -B^2/2) \quad e = \frac{1}{\sqrt{137}}$$

Gaussian units:

$$T_{\text{fields}}^{\mu\nu} = \text{diag}(B^2/8\pi, B^2/8\pi, B^2/8\pi, -B^2/8\pi) \quad e = \sqrt{\frac{4\pi}{137}}$$

$$n = \sum_s \int_k f, \epsilon = T^{00} = \sum_s \int_k E f, \quad (2)$$

$$P_{\parallel} = T^{zz} = \sum_s \int_k \frac{k_z^2}{E} f, \quad (3)$$

$$\begin{aligned} P_{\perp} &= \frac{1}{2} (T^{xx} + T^{yy}) \\ &= \sum_s \int_k \frac{1}{E} \left[\frac{1}{2} \frac{k_{\perp}^2 \bar{m}(\nu)}{\sqrt{m^2 + k_{\perp}^2}} - s\kappa B \bar{m}(\nu) \right] f, \end{aligned} \quad (4)$$

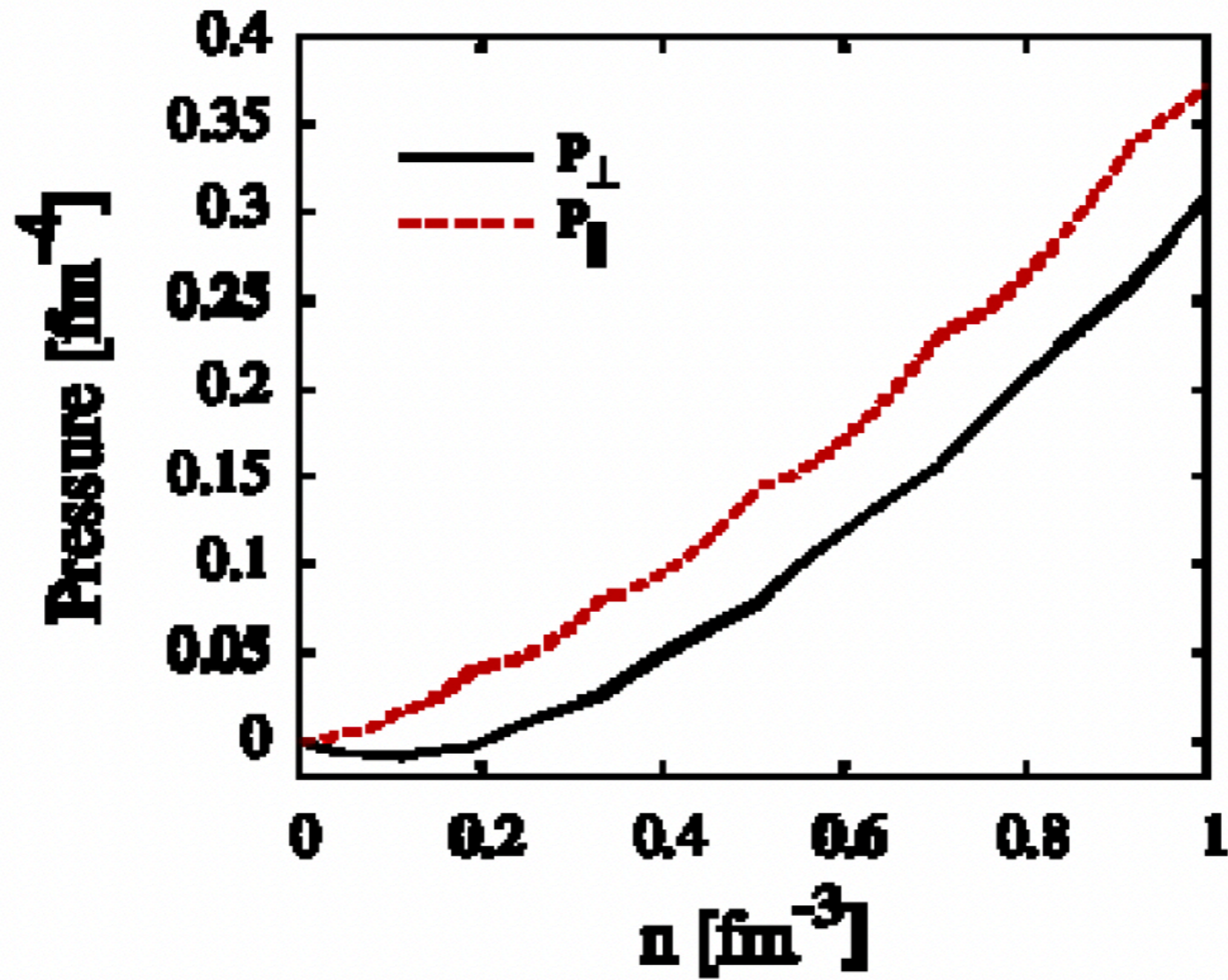
$$P_{\perp} = P_{\parallel} - MB$$

$$\bar{m}^2(\nu) \equiv (\sqrt{m^2 + k_{\perp}^2} - s\kappa B)^2, \quad \kappa - \text{AMM}$$

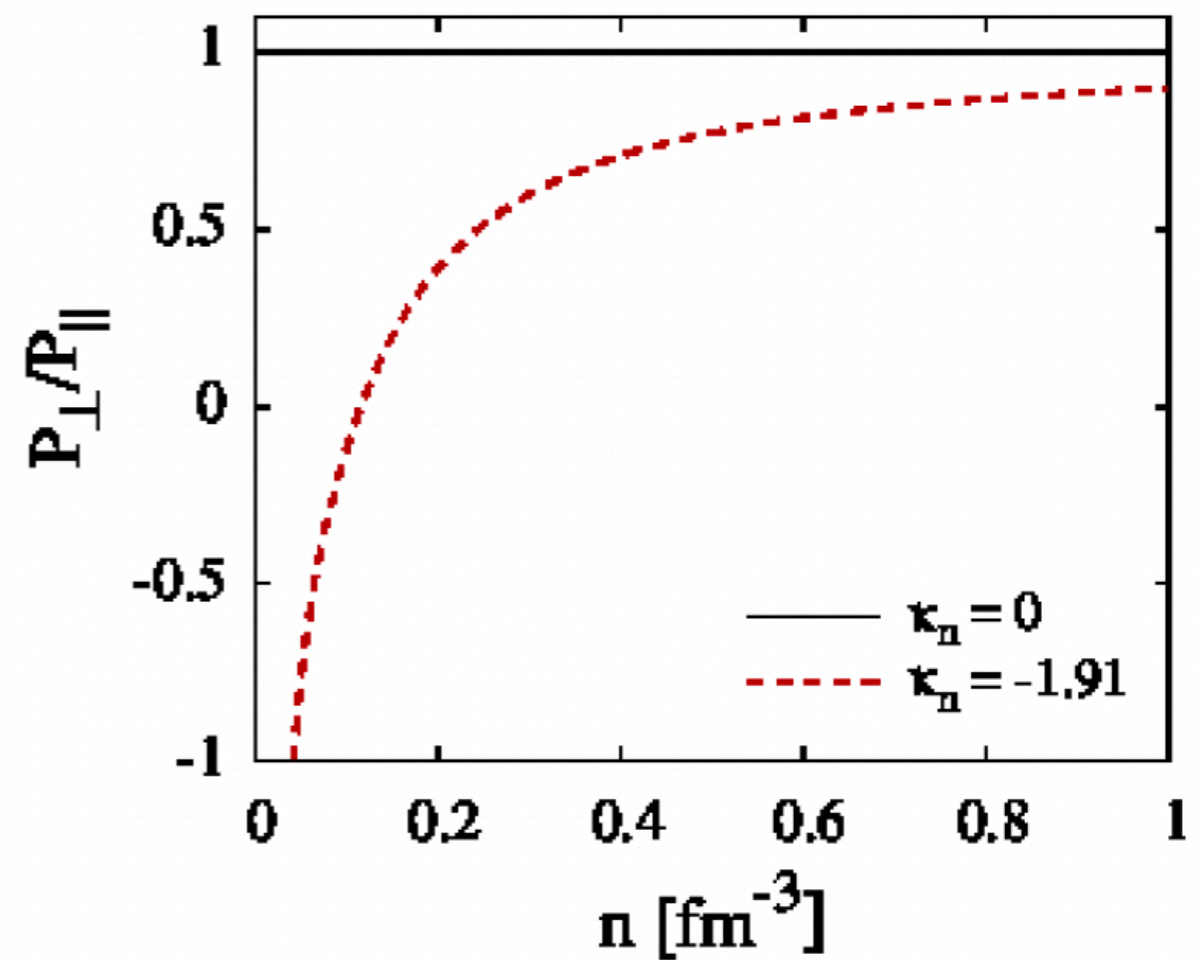
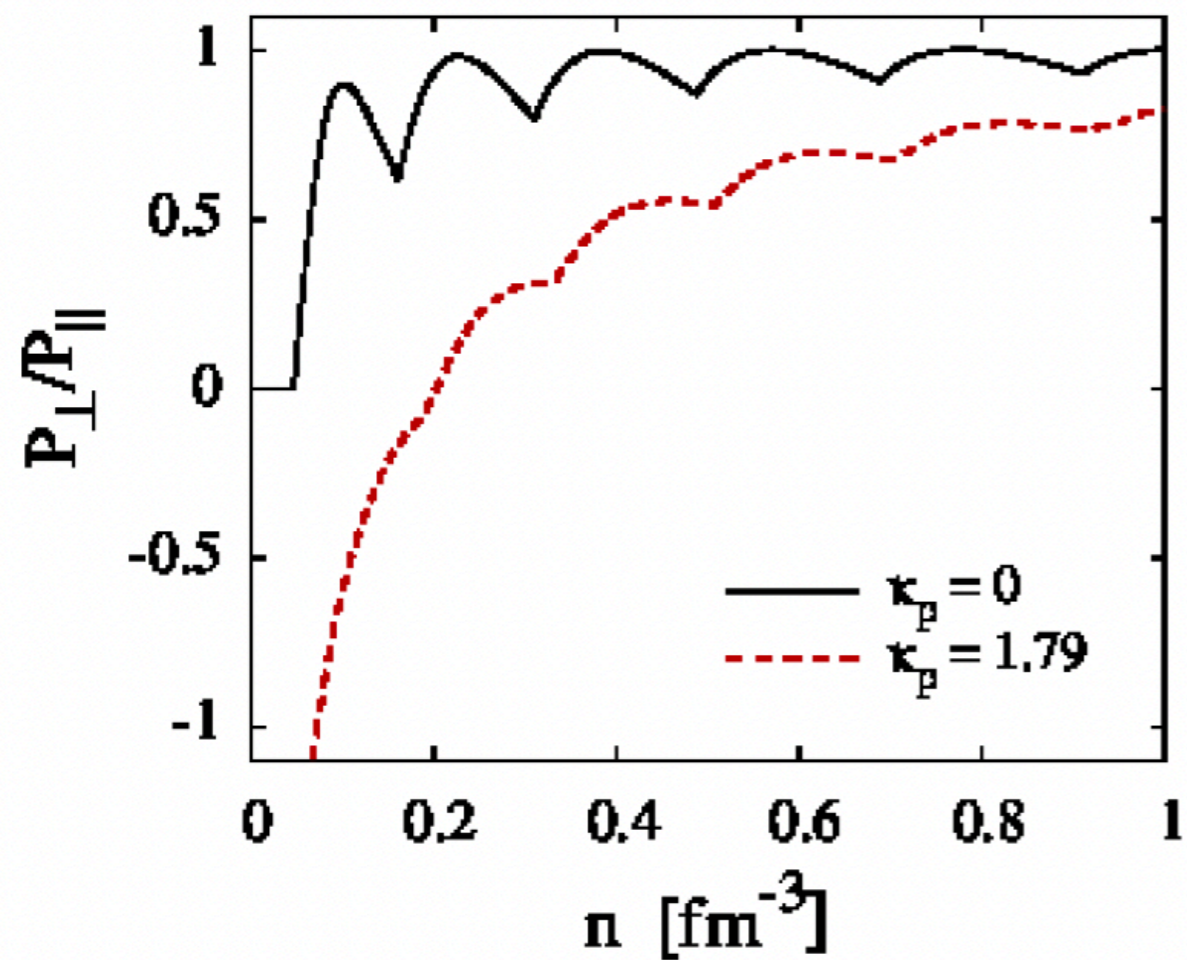
k_{\perp}^2 - (discretized) transverse momentum, \sum_s over spin polarizations

$$M = -\frac{\partial \Omega}{\partial B} = \frac{\partial P_{\parallel}}{\partial B} = \frac{P_{\parallel} - P_{\perp}}{B}$$

Proton and neutron gases

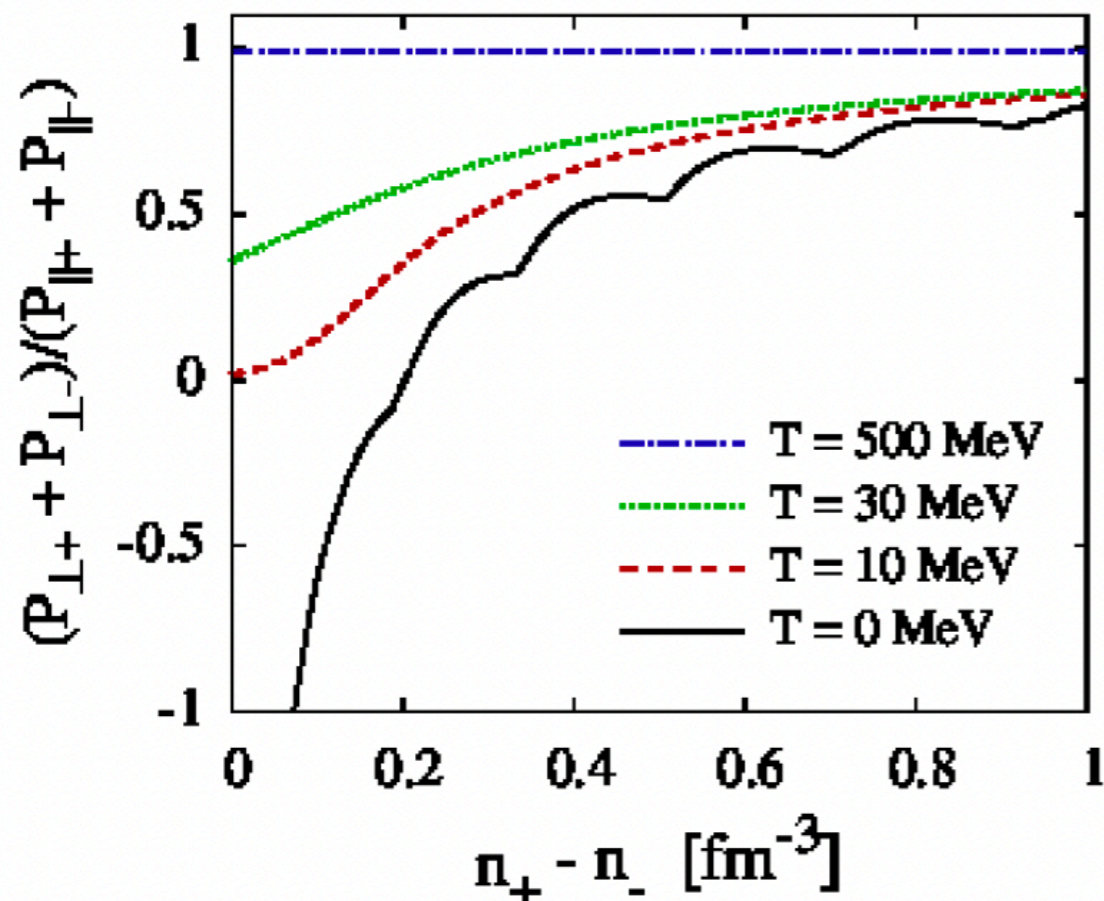


Transverse and longitudinal pressures of a gas of protons; $T=0$, with AMM; $B = 5 \times 10^{18}$ G; $P_{\perp} = P_{\parallel} - MB$.

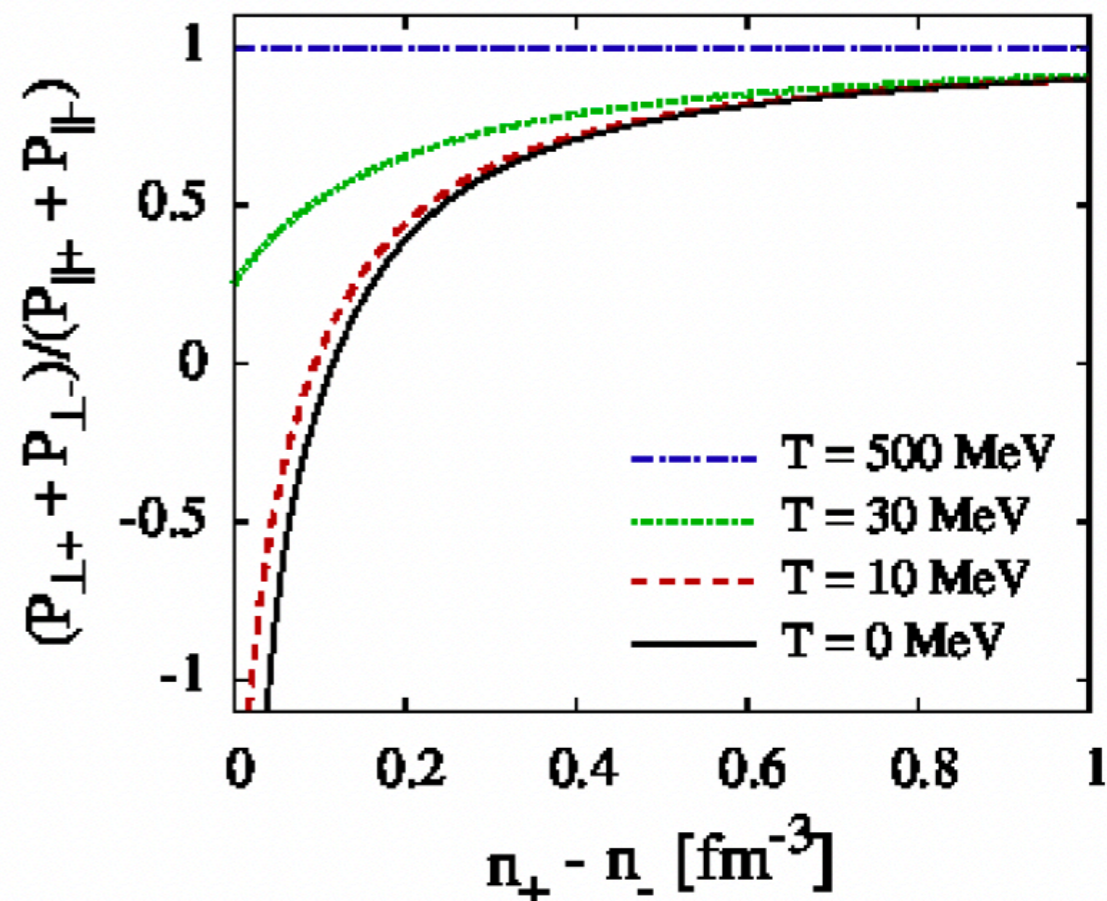


Ratio of transverse and longitudinal pressures: $T=0$; $B = 5 \times 10^{18}$ G;
 $P_{\perp} = P_{\parallel} - MB$.

Protons



Neutrons



Ratio of transverse to longitudinal pressure $T = \{0, 10, 30, 500\}$ MeV, with AMM; $B = 5 \times 10^{18}$ G; $P_{\perp} = P_{\parallel} - MB$.

M. Strickland, V. Dexheimer and D.P. Menezes, Phys. Rev. D 86, 125032 (2012)

How to deal with anisotropic effects on NS?

1) Ignore it and run TOV

$$P_{\text{iso}} = P_f + P_l + B(\epsilon)^2 / 2,$$

$$\epsilon_{\text{iso}} = \epsilon_f + \epsilon_l + B(\epsilon)^2 / 2.$$

2) Assume chaotic B and run TOV

O(3) rotation symmetry remains valid

$$P = \frac{1}{3} \langle T_i^i \rangle = \frac{1}{3} \left(\frac{B^2}{6} + \frac{B^2}{6} + \frac{B^2}{6} \right) = \frac{B^2}{6}.$$

3) Take anisotropy into account

$$P_{\parallel} = P_f + P_l - B(\epsilon)^2 / 2, \quad P_{\perp} = P_f + P_l - \mathcal{M}B + B(\epsilon)^2 / 2.$$

$$\mathcal{M} = dP/dB,$$

$$B(\epsilon) = B_0 \left(\frac{\epsilon_M}{\epsilon_0} \right)^\gamma + B^{\text{surf}};$$

B_0 is a fixed value, ϵ_0 at the centre of non-mag M_{max}

ϵ_M matter alone, γ is a positive number

But ...

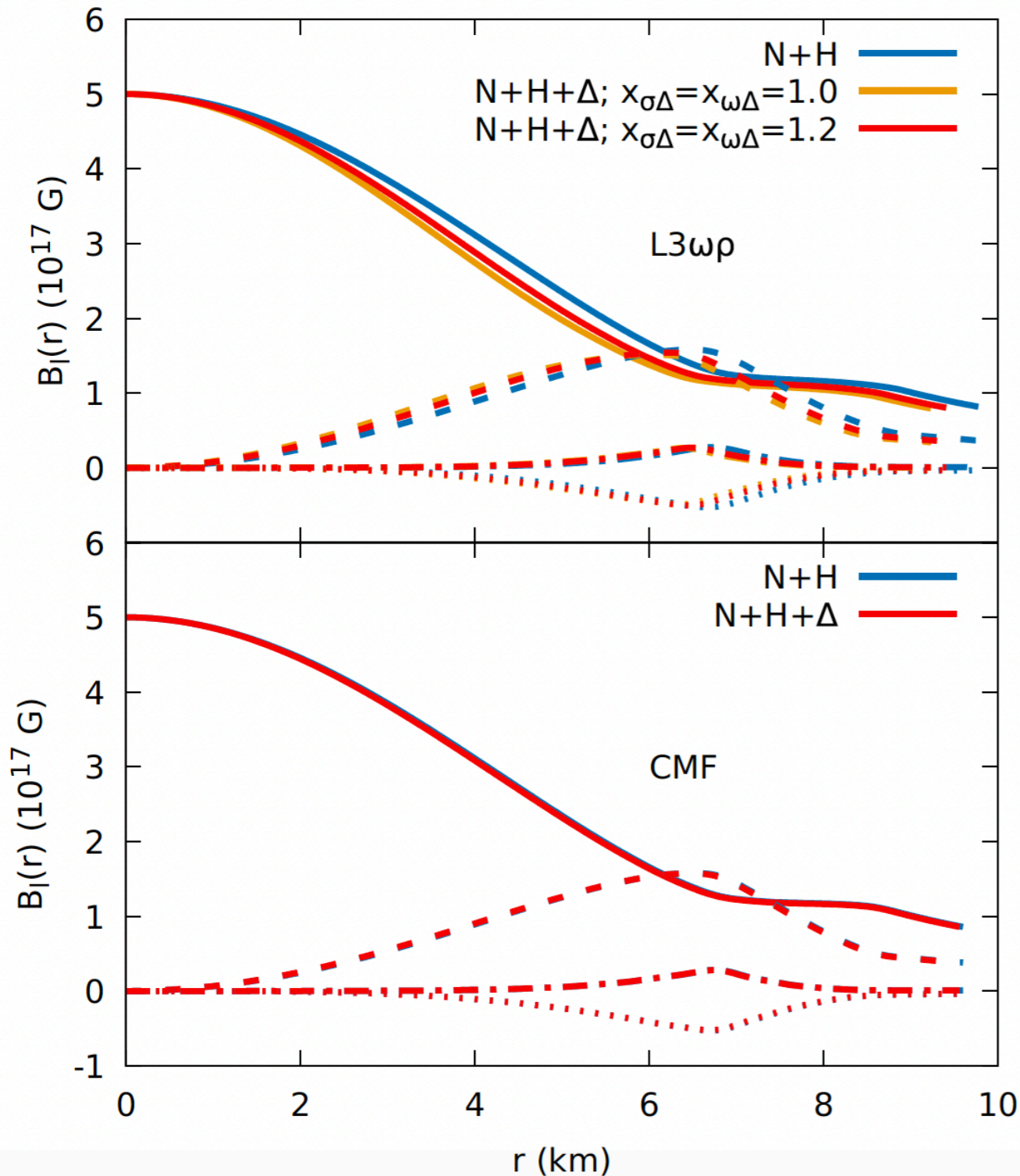
Maxwell Equation Violation by Density Dependent Magnetic Fields in Neutron Stars

$$B(r, \theta) \approx \sum_{i=0}^{l_{max}} B_l(r) Y_l^0(\theta),$$

LORENE - $l = 0, 2, 4, 6$

**Solid (monopolar), dashed (dipolar),
dash-dotted (quadrupolar), dotted**

**Magnetic distribution inside
a NS of $1.8 M_{\odot}$**



**K.D. Marquez, M.R.Pelicer, S. Ghosh, J.Petterson, D. Chatterjee, V. Dexheimer,
DPM, PRC 106, 035801 (2022)**

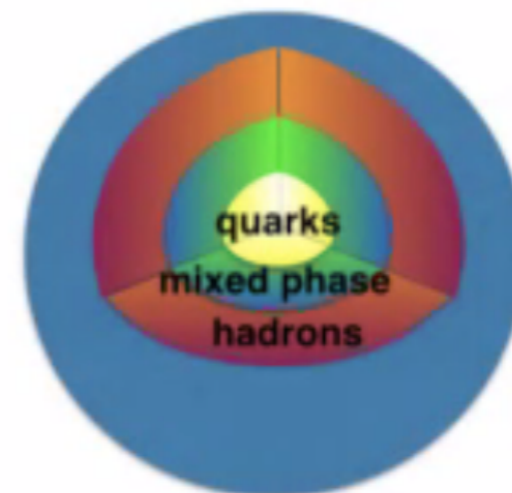
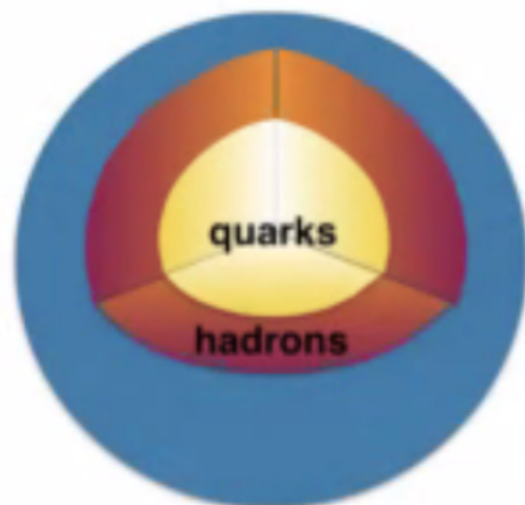
hybrid and quark stars

**1969 - hybrid stars (possible superconductor core)
Ivanenko + Kurdgelaidze**

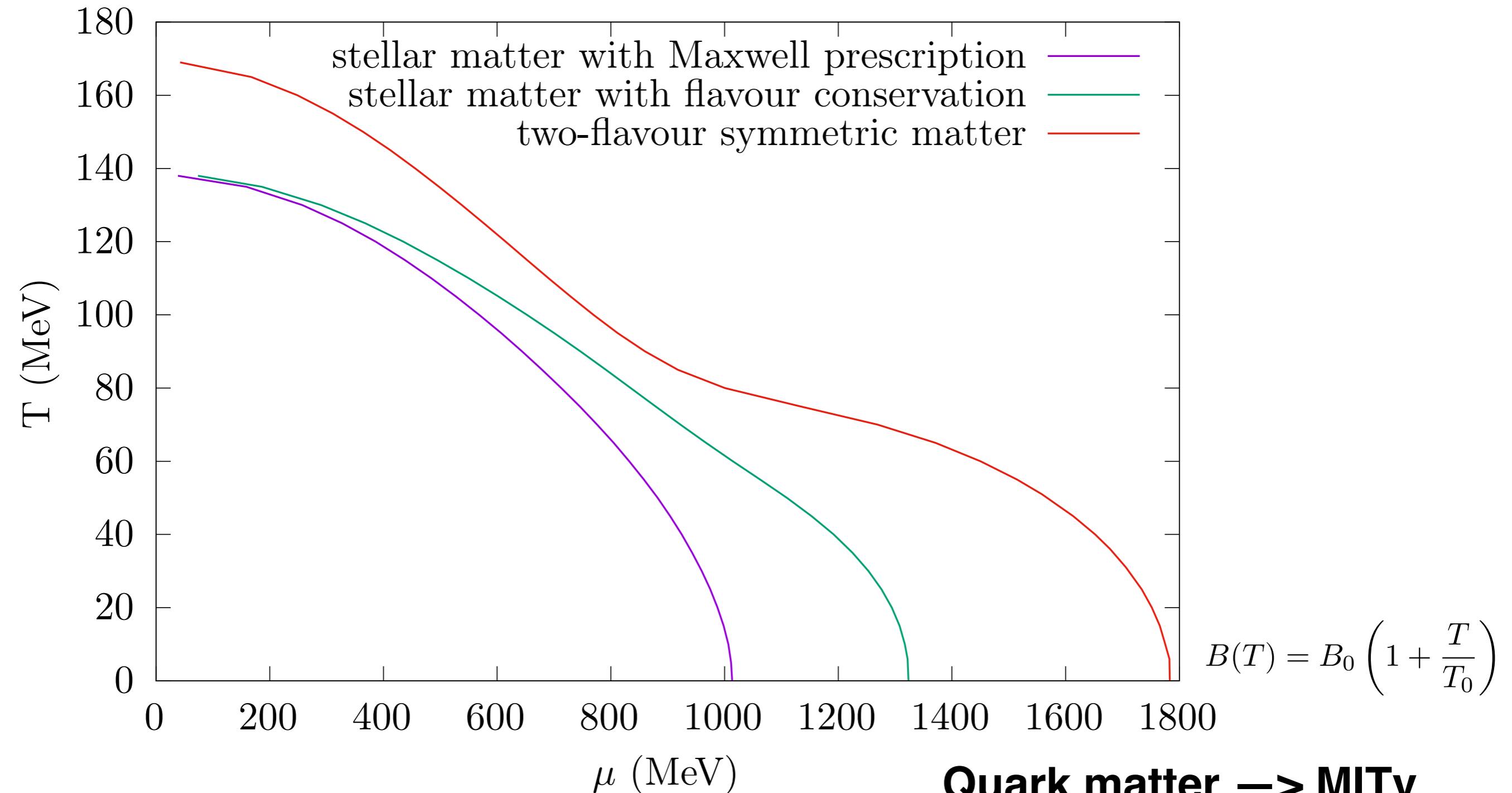
1970 - quark stars - Itoh

**Bodmer (1971) and Witten (1984) conjecture
strange stars**

hybrid stars - with or without mixed phase



QCD phase diagram (two models) - $B=0$



Hadronic matter \rightarrow e L3wr

Quark matter \rightarrow MITv

$$B_0^{1/4} = 165 \text{ MeV} \rightarrow T_0 = 155 \text{ MeV}$$

$$G_V = 0.1 \text{ fm}^2$$

Magnetized matter with flavor conservation, $T=0$

Betânia C.T. Backes, Kauan D. Marquez and DPM, EPJA (2021) 57:229

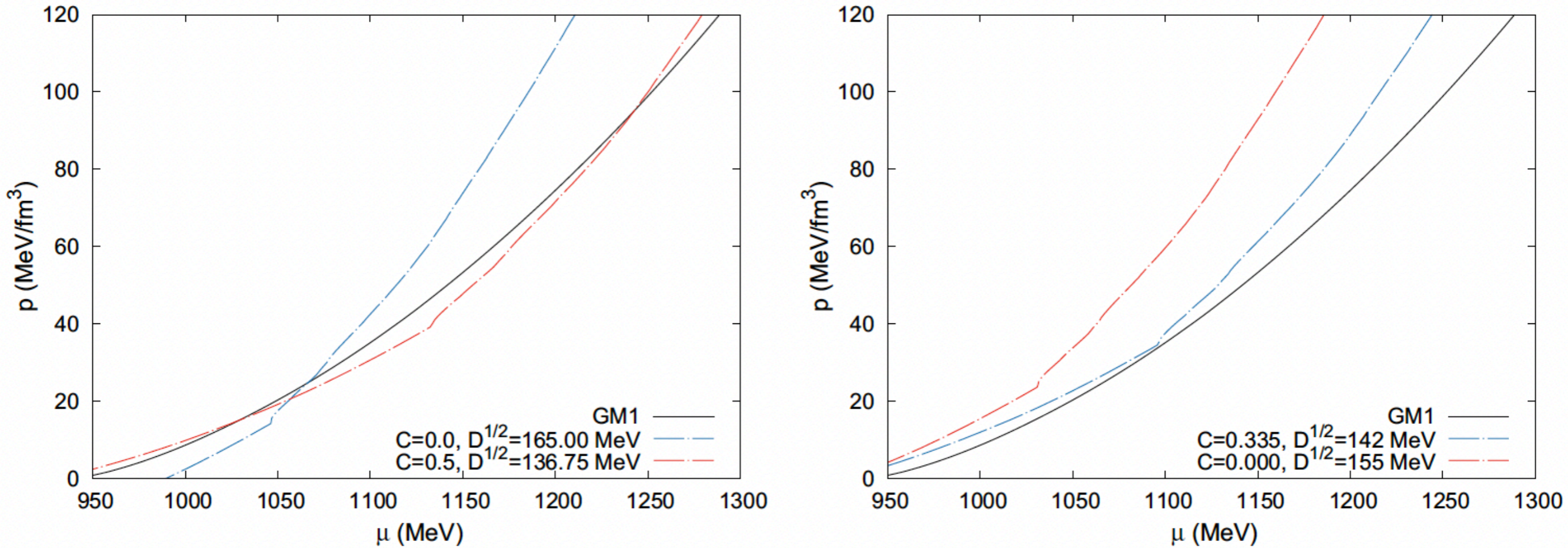
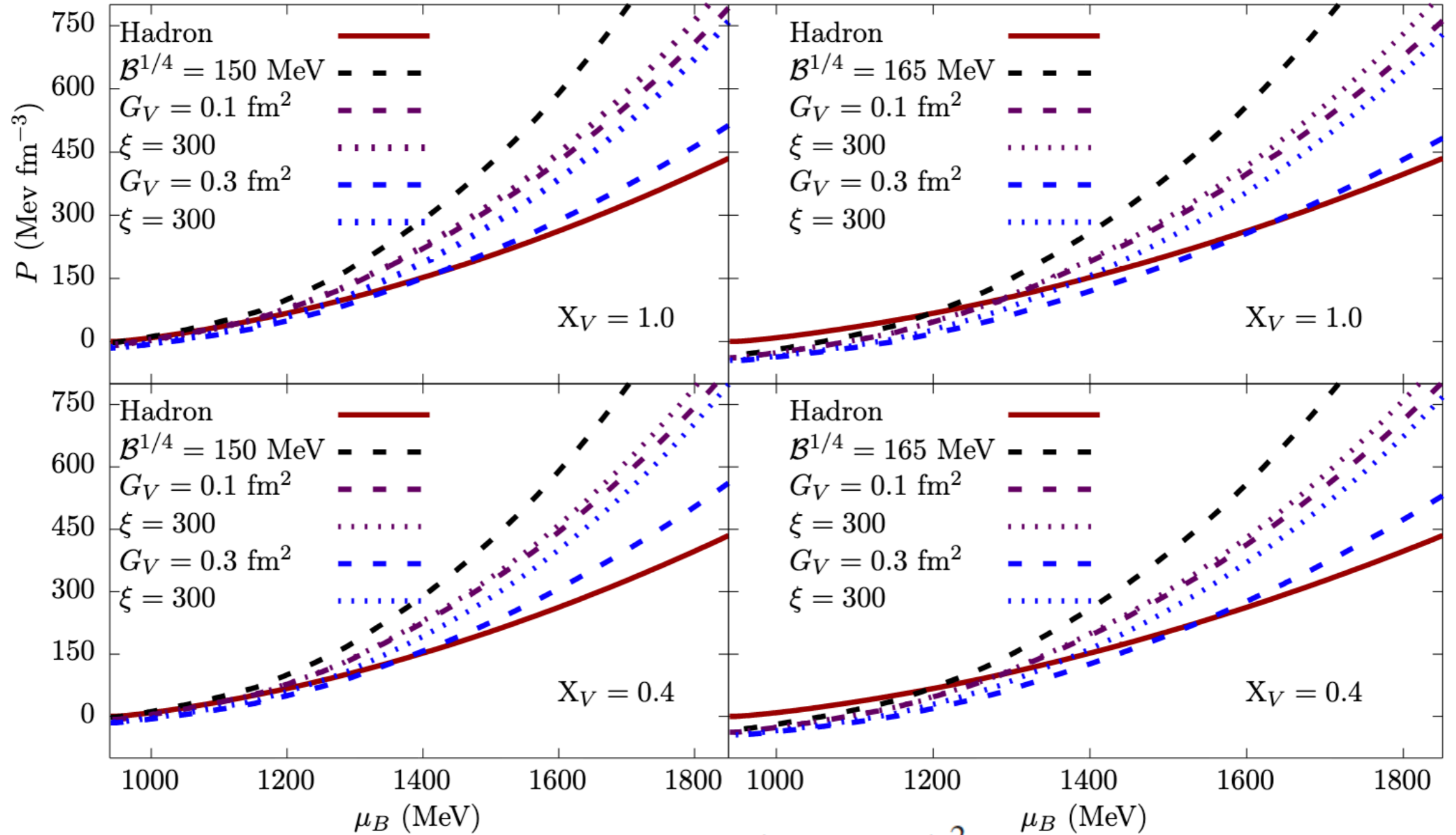


Fig. 2 Example of parameter sets that allow (left panel) and do not allow (right panel) the hadron-quark phase transition to occur at $B = 3 \times 10^{18}$ G

$$Y_q = \sum_b \frac{1}{3} N_{qb} Y_b,$$

Magnetized matter with flavor conservation, T=0

M.R.Pelicer and DPM EPJA (2022) 58:177



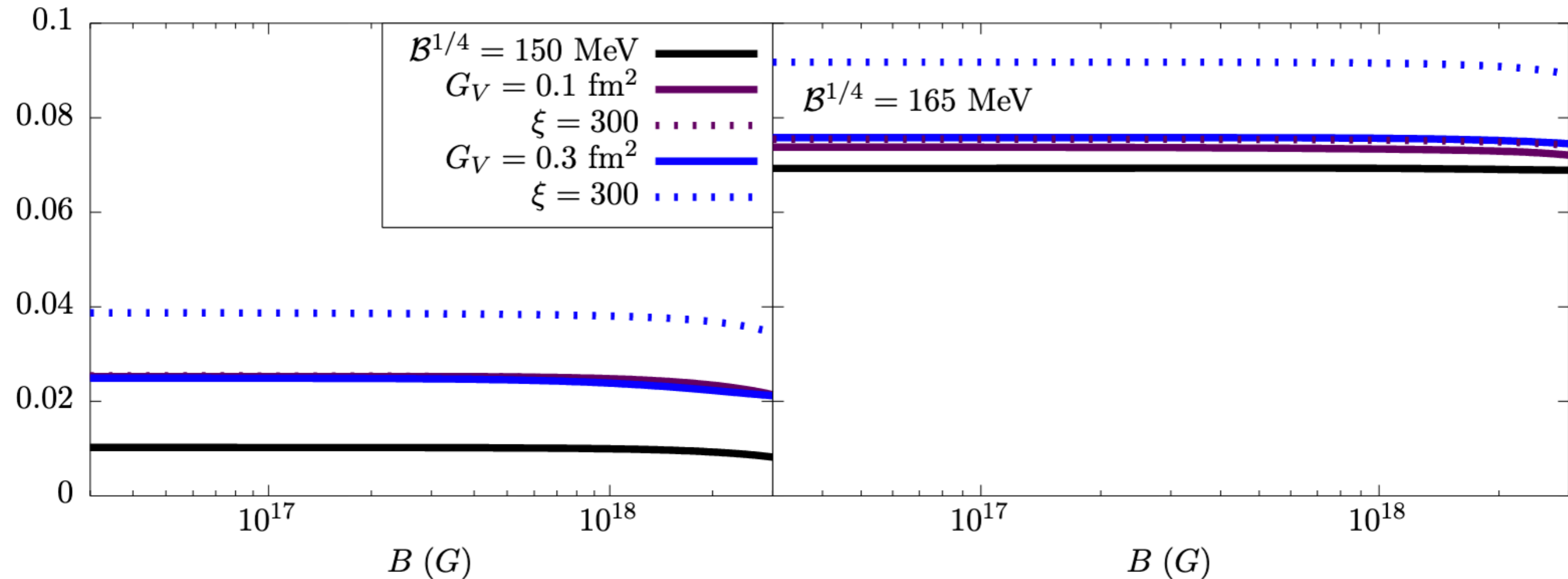
$$\mathcal{L}_{\text{Dirac}} = b_4 \frac{(g^2 V_\mu V^\mu)^2}{4}, \quad g = g_{uV} \quad b_4 = \xi$$

Hadronic matter - $NL3\omega\rho^*$

$B = 3 \times 10^{18} \text{ G}$

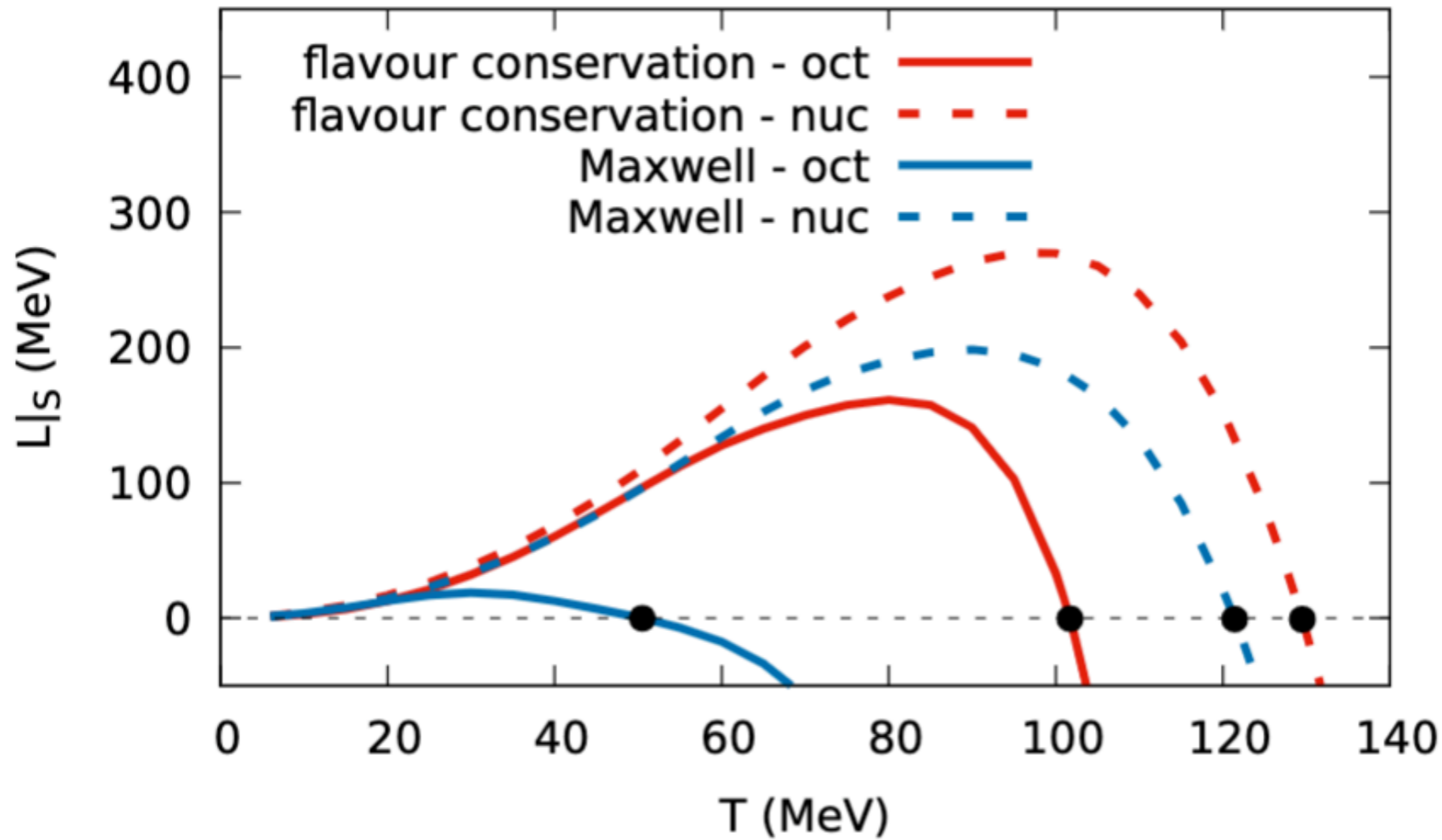
$$L|_{\varepsilon} = P_H \frac{\varepsilon_Q - \varepsilon_H}{\varepsilon_Q \varepsilon_H}$$

Latent energy



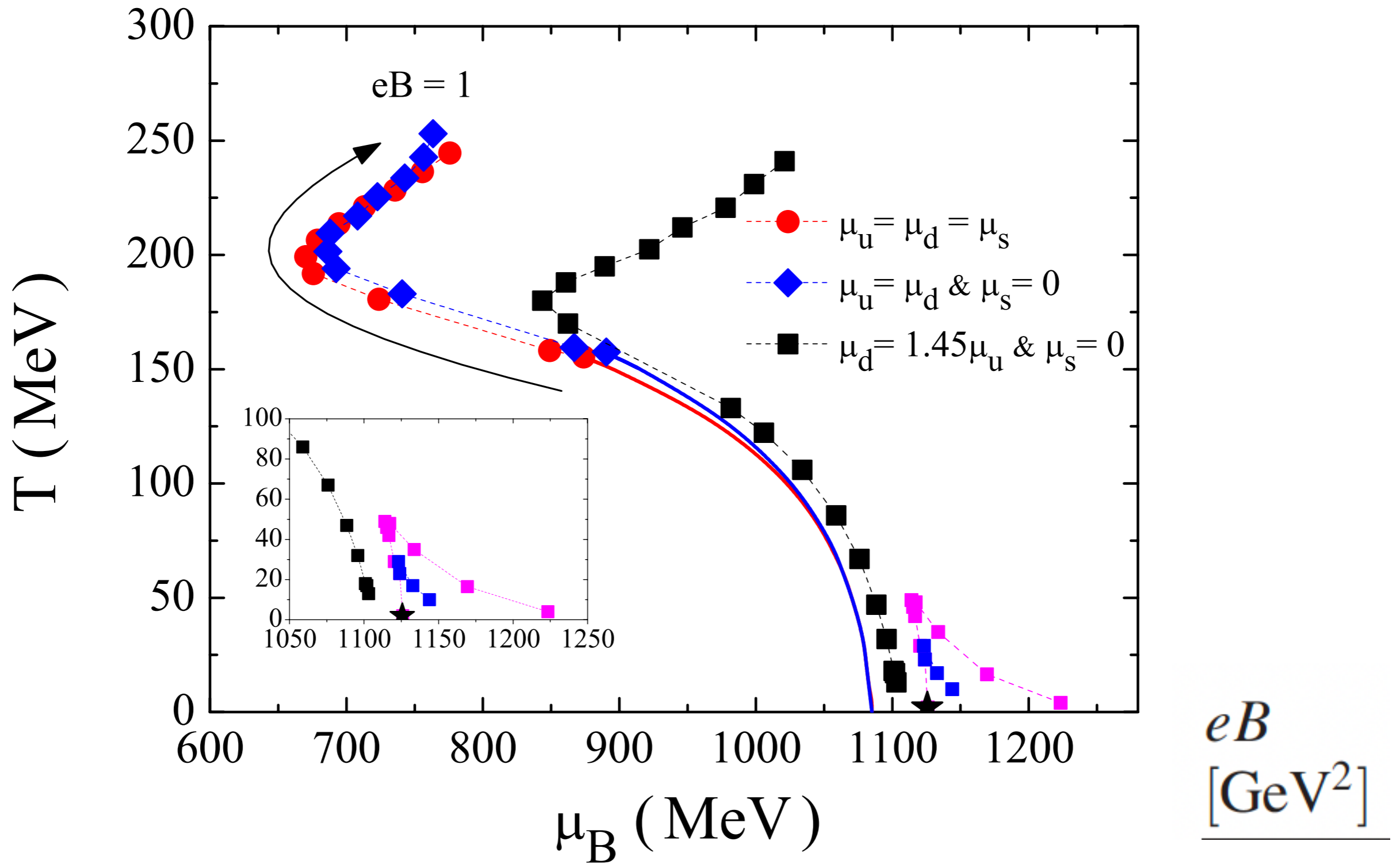
The value of the magnetic field where latent heat turns to zero corresponds to the CEP

Latent heat **B=0**



$$L|_S = (S^Q - S^H) T,$$

Carline Biesdorf, Luiz L. Lopes and DPM, BJP (2023) 53:137



**Can we reproduce this behavior with 2 models?
2CEPs at low T and strong B (pink and blue)**



Thank you !

Constança Providência, Francesca Gulminelli, Mariana Dutra,
Odilon Lourenço, Luiz L. Lopes, Verônica Dexheimer,
Mateus Pelicer, Norberto Scoccola,
Kauan D. Marquez, Carline Biesdorf,
many students



Charged particles

$$\int_k \rightarrow \frac{|q|B}{(2\pi)^2} \sum_n \int_{-\infty}^{\infty} dk_z, \quad (5)$$

$$\nu = n + \frac{1}{2} - \frac{s q}{2|q|}, s = \pm 1, \quad \text{spin } 1/2 \text{ particles} \quad (6)$$

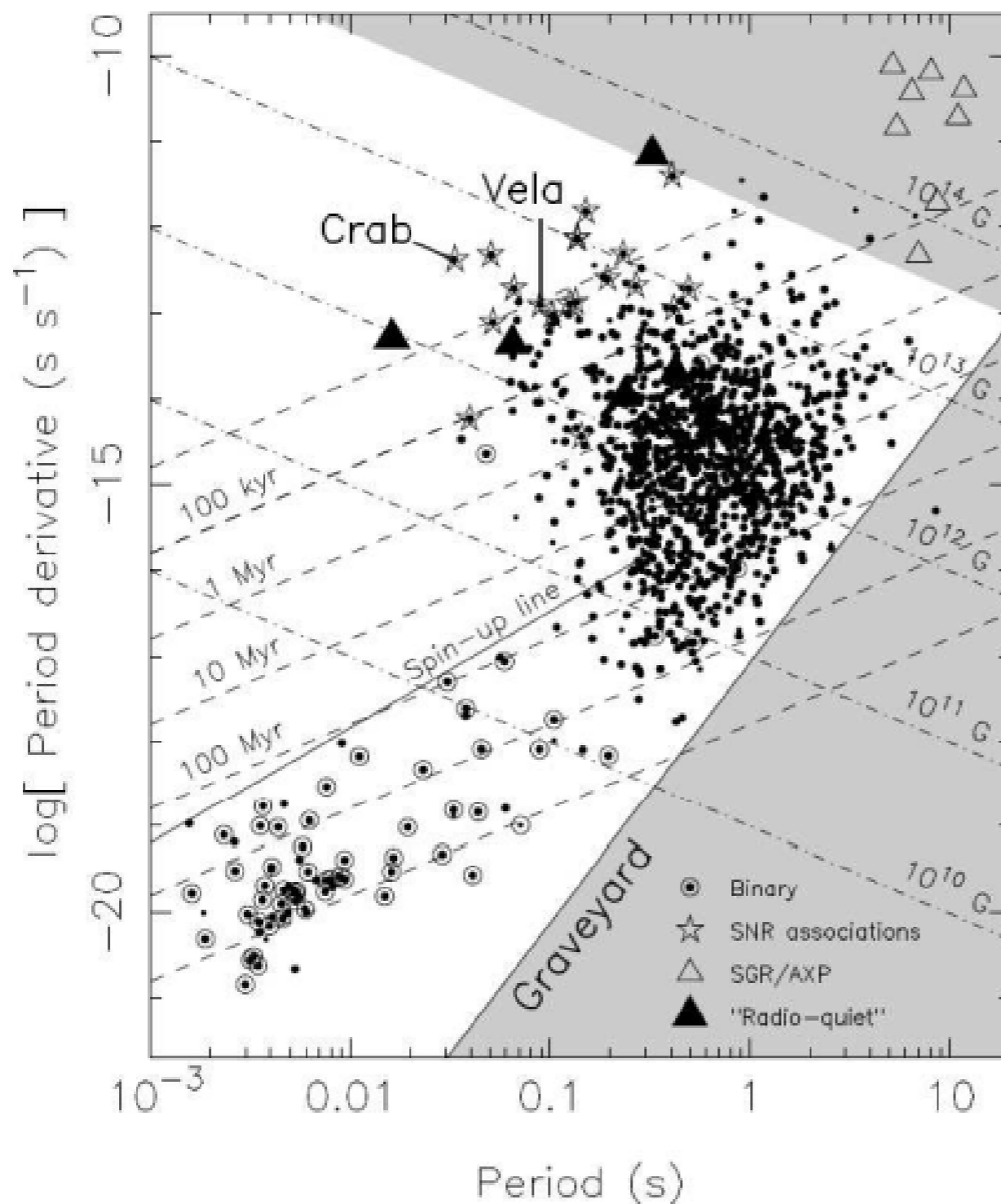
$$E = \sqrt{k_z^2 + \bar{m}^2(\nu)}, \quad \bar{m}^2(\nu) \equiv (\sqrt{m^2 + 2\nu|q|B} - s\kappa B)^2 \quad (7)$$

Uncharged particles

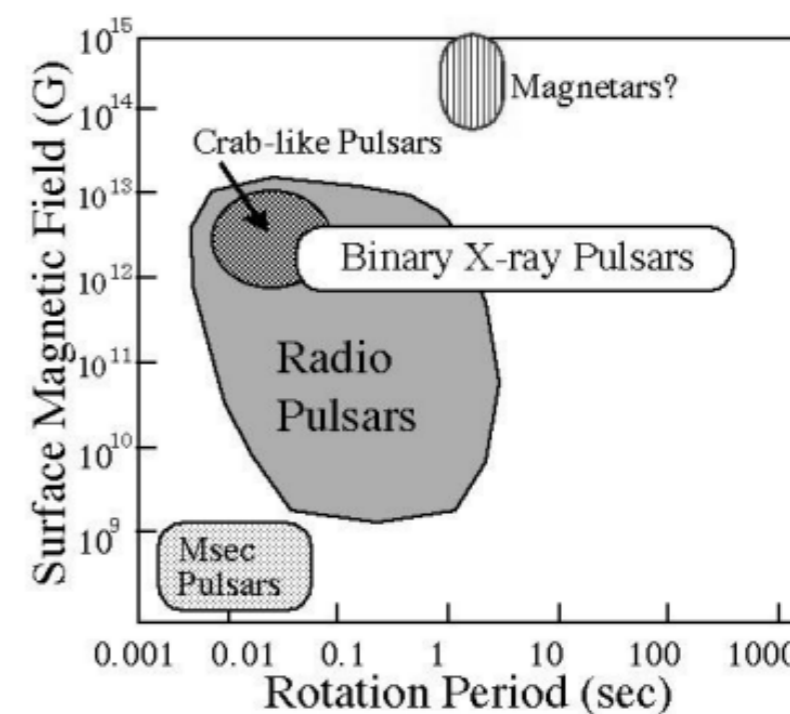
$$\int_k \rightarrow \int \frac{d^3k}{(2\pi)^3}, \quad (8)$$

$$\bar{m} = (m - s\kappa B). \quad (9)$$

Magnetic field and spin down



$$B_0 = \left(\frac{3Ic^3 P \dot{P}}{8\pi^2 R_0^6} \right)^{1/2}$$



- ◆ $P = 2 - 12s$
- ◆ $\dot{P} = 10^{-13} - 10^{-10}$
- ◆ $L = 10^{33} - 10^{36} \text{ erg/s}$

Source: Makishima, K., Progress of Theoretical Physics Supp. No. 151, 2003

H.Müller and B. Serot,
 Phys. Rev. C 52, 2072 (1995)

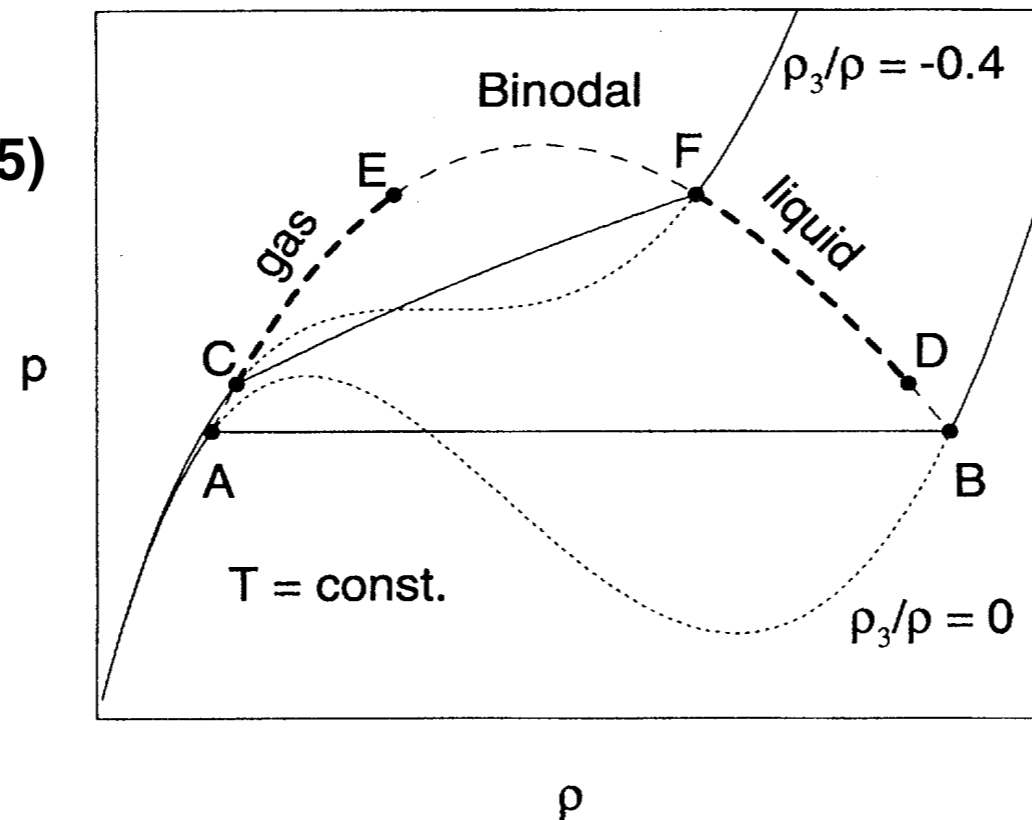
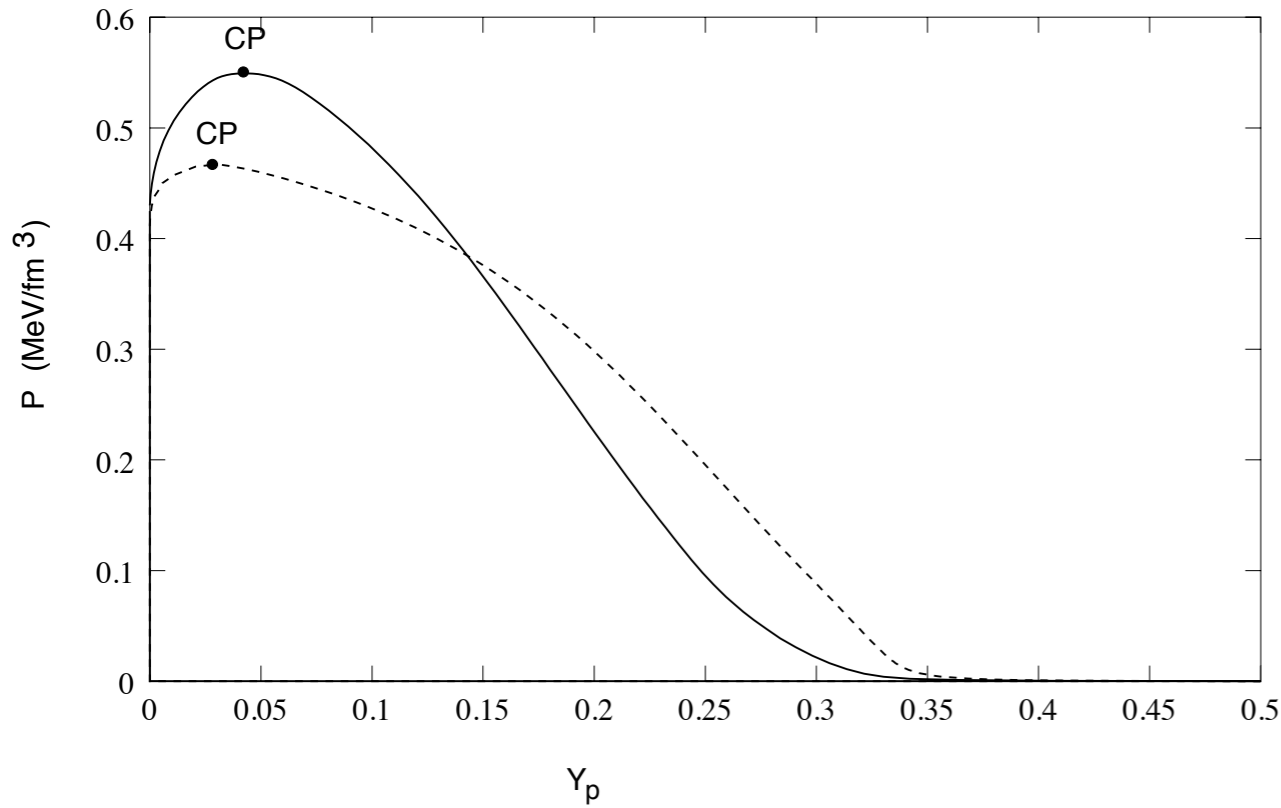


FIG. 3. The Maxwell construction for symmetric and asymmetric systems. The construction for symmetric matter ($\rho_3/\rho=0$) is indicated by the segment AB and is the same as for a one-component system. The construction for asymmetric matter with $\rho_3/\rho=-0.4$ is indicated by the segment CF and shows the qualitatively new behavior allowed in a two-component system. The asymmetry is held constant throughout the phase separation. The (dashed) binodal line is obtained from similar isotherms at other values of the asymmetry.

Phase Transitions in multicomponent systems:

$K_{\max}=n+2$ phases can coexist in a system with n conserved charges (more than 2 phases can coexist if and only if each pair of phases form a binodal and if all the binomials have a common region of intersection.

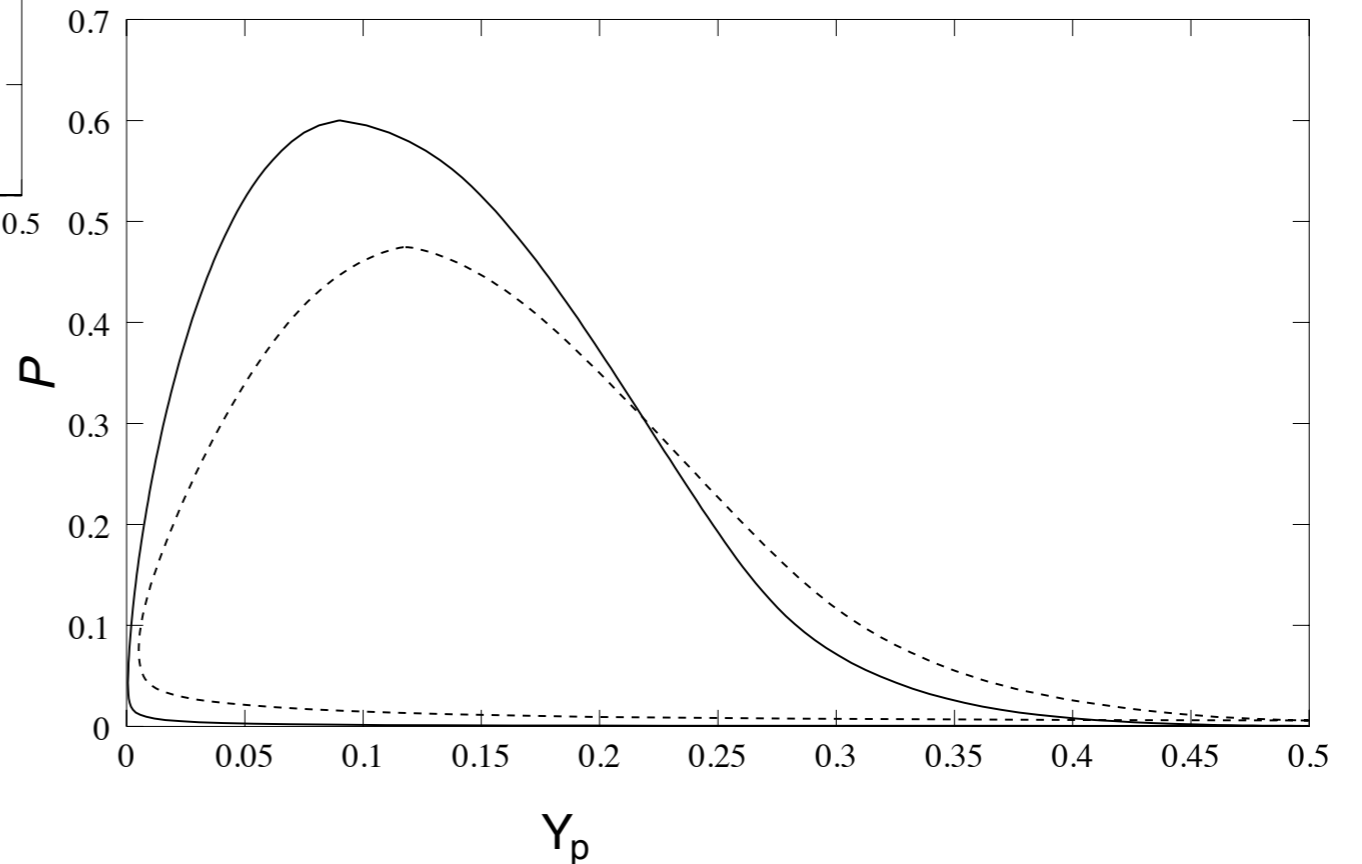
- **Binodal sections** - obtained from the conditions of phase coexistence:



T=0

solid - QMC
dashed - NL1

solid- T=5 MeV
dashed - T=7.5 MeV



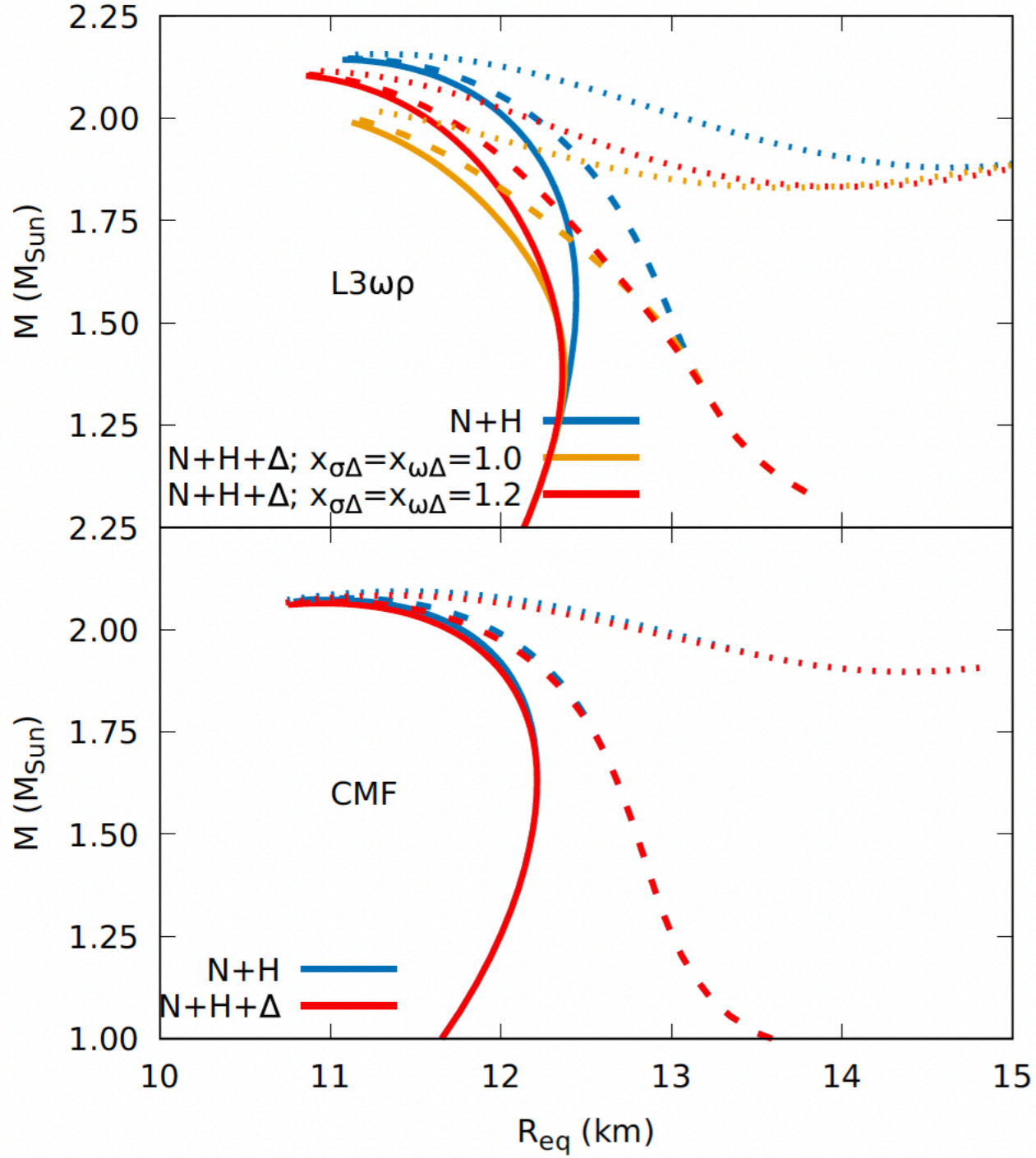


FIG. 7. Stellar mass as a function of equatorial radius for different compositions and interaction strengths, for central magnetic fields $B = 0$ (solid lines), $B = 5 \times 10^{17}$ G (dashed lines), and $B = 10^{18}$ G (dotted lines). The top and bottom panels show results for the L3 $\omega\rho$ and CMF models, respectively.

Results obtained with the LORENE code

TABLE II. Central baryon (n_c) and energy (ε_c) densities as a function of magnetic field strength for neutron stars of radius 12 km with the L3 $\omega\rho$ model for $x_{\sigma\Delta} = x_{\omega\Delta} = 1.0(1.2)$ in the top panel and the CMF model in the bottom panel.

B (G)	n_c (fm^{-3})		ε_c (MeV/fm^3)	
	$N + H$	$N + H + \Delta$	$N + H$	$N + H + \Delta$
0	0.672	0.618 (0.614)	742	658 (657)
5×10^{17}	0.701	0.659 (0.653)	783	712 (708)
1×10^{18}	0.747	0.714 (0.707)	850	786 (783)
0	0.629	0.625	678	672
5×10^{17}	0.680	0.677	747	741
1×10^{18}	0.749	0.746	843	837

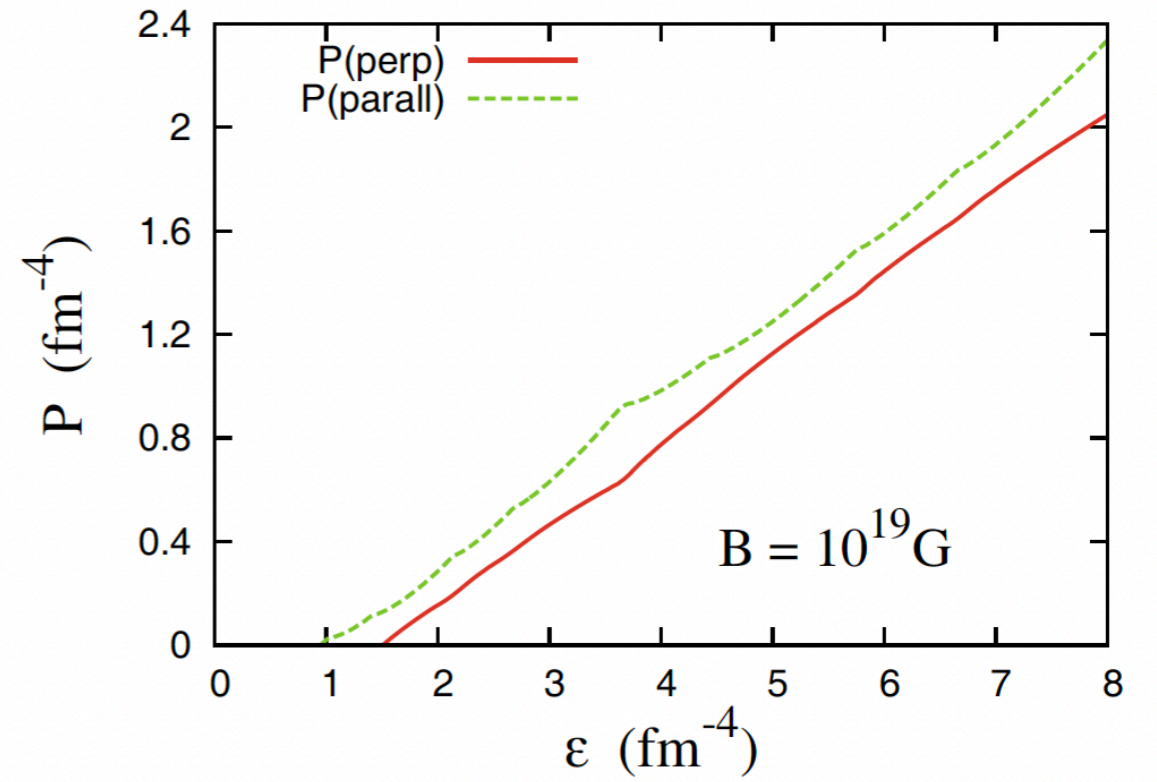
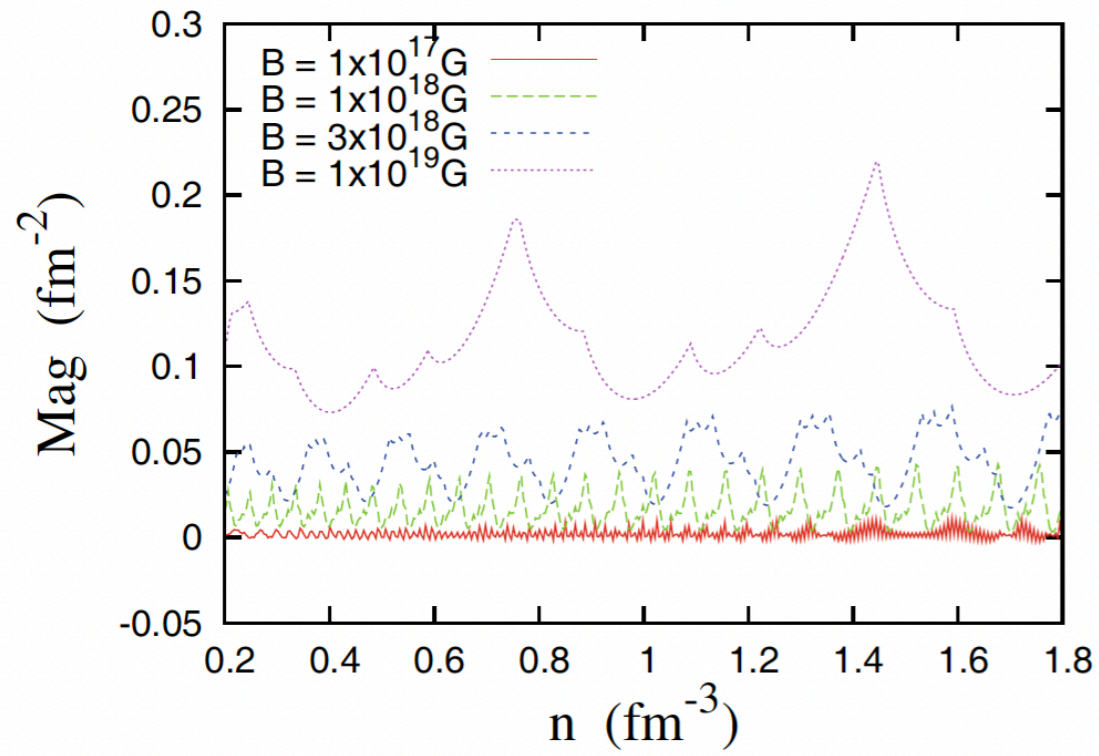


Fig. 4. MIT bag model EOS obtained for $B = 10^{19}$ G without the term proportional to B^2 .

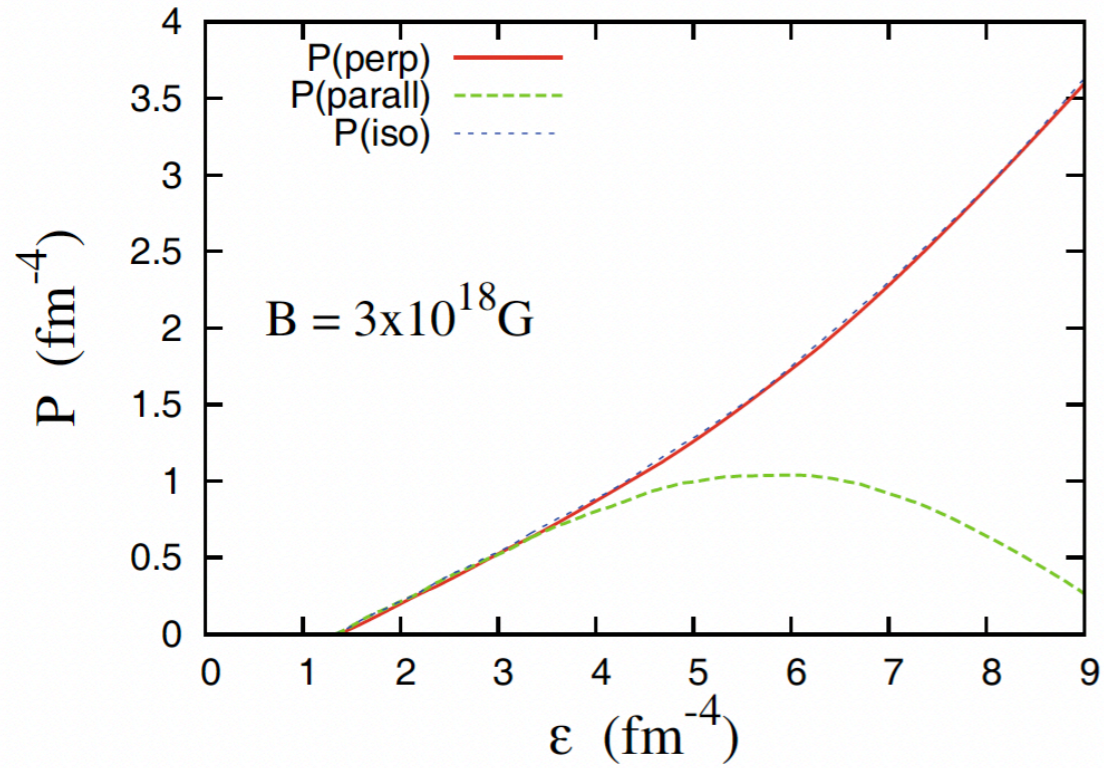


Fig. 6. MIT bag model EOS obtained for $B = 3 \times 10^{18}$ G with the term proportional to B^2 .

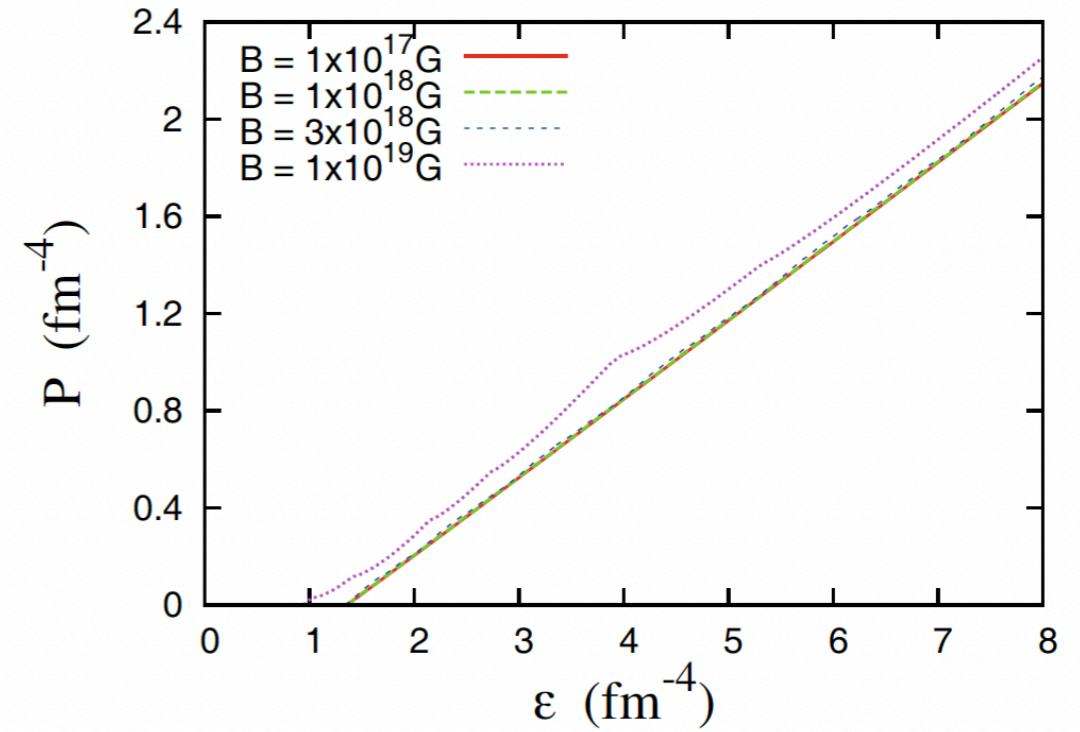


Fig. 8. MIT bag model EOS for different values of the chaotic magnetic field.

